Supporting information for *INFLUENCE OF SUBSTITUENTS IN ARYL GROUPS ON THE STRUCTURE AND THERMAL TRANSITIONS OF ZINC BIS(DIARYLPHOSPHATE) HYBRID POLYMERS*

Supporting Information for

INFLUENCE OF SUBSTITUENTS IN ARYL GROUPS ON THE STRUCTURE, THERMAL TRANSITIONS AND ELECTRORHEOLOGICAL PROPERTIES OF ZINC BIS(DIARYLPHOSPHATE) HYBRID POLYMERS

Maciej Dębowski,* Piotr A. Guńka,* Konrad Żurawski, Magdalena Zybert, Beata Modzelewska, Andrzej Ostrowski, Janusz Zachara, Zbigniew Florjańczyk

Faculty of Chemistry, Warsaw University of Technology, Noakowskiego 3, 00-664 Warsaw, Poland.

Inorganic–organic hybrid polymer, metal organophosphate, zinc diarylphosphate, electrorheology

TABLE OF CONTENT

corresponding authors: maciej.debowski@pw.edu.pl; piogun@ch.pw.edu.pl

corresponding authors: maciej.debowski@pw.edu.pl; piogun@ch.pw.edu.pl

Synthesis of phosphoric acid triester containing *p*-$C_6H_4NO_2$ groups

The reaction was carried out in a 250 mL round bottom flask equipped with a dropping funnel, reflux condenser, thermometer and mechanical stirrer. A general procedure was as follows: 4-nitrophenol (21.07 g, 151.5 mmol), benzyltriethylammonium chloride (1,12 g, 4.9 mmol) and 100 mL of dichloromethane were vigorously mixed with a solution of NaOH (6.28 g, 157.0 mmol) in 60 mL H_2O. Subsequently, the dispersion was cooled to −5–0 °C and $POCl_3$ (4,5 mL, 48.3 mmol) was added dropwise *via* dropping funnel. The reaction was carried out for another 10 minutes at −5–0 °C, and then slowly warmed up to room temperature. Dichloromethane was removed on a rotary evaporator, followed by dispersing the non-volatile residue in 100 mL of water and separation of its water-insoluble fraction *via* filtration under reduced pressure. In a vacuum oven (*ca*. 1×10^{-2} mbar) all volatiles were removed from the resulting raw product, which was furtherly purified by recrystallization from 40 mL of acetone giving 18.20 g of Tris(4-nitrophenyl) phosphate (reaction yield 81%).

Tris(4-nitrophenyl) phosphate: Melting temperature: 152.1–153.9 °C. Elemental anal.: C 46.90%, H 3.18% (calculated for $C_{18}H_{12}N_3O_{10}P$: C 46.87%, H 2.62%). FT-IR (neat, cm^{-1}):* 3117 (vw), 3080 (vw), 1614 (m), 1588 (m), 1519 (m), 1483 (m), 1371 (vw), 1346 (s), 1304 (m), 1235 (w), 1187 (s), 1154 (s). 1108 (m), 1097 (m), 1010 (w), 963 (s), 948 (vs), 926 (s), 852 (vs), 823 (m), 813 (m), 771 (s), 748 (vs), 736 (m), 683 (s), 642 (s), 627 (m), 616 (s), 601 (m), 546 (s), 532 (m), 517 (s), 494 (m), 466 (s), 445 (vs), and 405 (s). ^{1}H NMR (500 MHz, DMSO-d_6, residual solvent): δ_H 8.40–8.27 (2H, m, 3-H and 5-H), 7.70–7.55 ppm (2 H, m, 2-H and 6-H). ^{31}P NMR (202 MHz, DMSO-d_6, 85% H_3PO_4): δ_P −19.91 (s).

*abbreviations describing FT-IR bands: s – strong, m – medium, w – weak, v – very, sh – shoulder, br – broad.

Synthesis of phosphoric acid triesters containing *p*-$C_6H_4OCH_3$ or *p*-$C_6H_4C(O)OC_2H_5$ groups

General procedure

Triaryl phosphates were obtained in the reaction of phosphorus(V) oxychloride with an appropriate 4-substituted phenol (4-methoxyphenol or ethyl 4-hydroxybenzoate), in the presence of benzyltriethylammonium chloride (**TEBACl**) as a phase transfer catalyst. The reaction was carried out in a 500 mL round bottom flask equipped with a dropping funnel, reflux condenser, thermometer and mechanical stirrer. A general procedure was as follows: phenol (3.1 molar equivalent) and TEBACl (0.03 molar equivalent) were dissolved in 210 mL of dichloromethane at room temperature. To the resulting mixture a 30 wt% aqueous solution of NaOH (3.2 molar equivalent) was slowly added and the mixture was cooled to −5–0 °C. Subsequently, $POCl_3$ (1 molar equivalent) was added dropwise *via* dropping funnel while maintaining a vigorous mixing. The reaction was kept at −5–0 °C for 30 minutes, slowly warmed up to room temperature and then mixed for another 5 hours. Afterwards, 60 mL of a redistilled water was added dropwise and the vigorous mixing was kept for another 1 h. The resulting two immiscible clear liquids were separated on a separating funnel, and the organic layer was concentrated on a rotary evaporator. The residue was dissolved in 200 mL of ethyl acetate followed by extraction with: 1M HCl_{aq} (1 × 100 mL), H_2O (3 × 100 mL), 10 wt% aqueous solution of NaOH (1 × 100 mL) and H_2O

corresponding authors: maciej.debowski@pw.edu.pl; piogun@ch.pw.edu.pl

(3 × 100 mL). The purified organic layer was dried over anhydrous $MgSO_4$ and then concentrated on a rotary evaporator at 60 °C giving raw triaryl phosphate as a residue. All volatiles were removed from the latter by heating it for several hours at 60 °C under high vacuum (*ca*. 1×10^{-2} mbar). In that manner the following compounds were synthesized:

Tris(4-methoxyphenyl) phosphate. Reactants: $POCl_3$ (6.0 mL, 64.4 mmol), TEBACl (0.46 g, 2.0 mmol), 4-methoxyphenol (24.80 g, 199.8 mmol), NaOH (8.26 g, 206.5 mmol). Product: 22.90 g (yield 85%). Elemental anal.: C 59.74%, H 5.85% (calculated for $C_{21}H_{21}O_7P$: C 60.58%, H 5.08%). FT-IR (neat, cm^{-1}):* 3344 (vw,br), 3115 (vw), 3074 (vw), 3002 (vw), 2954 (vw), 2935 (vw), 2908 (vw), 2836 (vw), 1595 (vw,sh), 1498 (vs), 1463 (w), 1441 (w), 1361 (vW), 1292 (w), 1249 (w), 1218 (w), 1173 (vs), 1102 (w), 1029 (m), 1009 (w), 954 (vs,sh), 827 (s), 799 (w), 732 (w), 719 (w), 701 (w), 637 (w), 561 (w), 515 (m), and 471 (w). ^{1}H NMR (500 MHz, DMSO-d_6, residual solvent): δ_H 7.17–7.12 (2 H, m, 2-H and 6-H), 6.97–6.93 (2 H, m, 3-H and 5-H), 3.73 (3 H, s, Me). ^{31}P NMR (202 MHz, DMSO-d_6, 85% H_3PO_4): δ_P −15.81 (s).

Tris[4-(ethoxycarbonyl)phenyl] phosphate. Reactants: $POCl_3$ (6.0 mL, 64.4 mmol), TEBACl (0.44 g, 1.9 mmol), ethyl 4-hydroxybenzoate (33.50 g, 201.6 mmol), NaOH (8.23 g, 205.8 mmol). Product: 30.36 g (yield 87%). Melting temperature: 83.5–84.9 °C. Elemental anal.: C 60.19%, H 5.78% (calculated for $C_{27}H_{27}O_{10}P$: C 59.78%, H 5.02%). FT-IR (neat, cm^{-1}): 3108 (vw), 3064 (vw), 2982 (vw), 2938 (vw), 2903 (vw), 2874 (vw), 1715 (vs), 1599 (m), 1499 (m), 1476 (w), 1465 (w), 1446 (vw), 1414 (w), 1393 (vw), 1365 (w), 1305 (w), 1269 (vs), 1190 (s), 1157 (s), 1108 (m), 1096 (s), 1018 (m), 959 (vs), 931 (s), 859 (m,sh), 792 (w), 769 (s,sh), 691 (m), 636 (m), 624 (m), 598 (w), 547 (m), 533 (m), 506 (m), 483 (w), 468 (m), 445 (w), and 411 (w). ^{1}H NMR (500 MHz, DMSO-d_6, residual solvent): δ_H 8.06–8.01 (2 H, m, 3-H and 5-H), 7.47–7.43 (2 H, m, 2-H and 6-H), 4.30 (2 H, q, J = 7.1 Hz, CH_2CH$_3$), 1.30 (3 H, t, J = 7.1 Hz, CH$_2$CH_3). ^{31}P NMR (202 MHz, DMSO-d_6, 85% H_3PO_4): δ_P −19.13 (s).

*abbreviations describing FT-IR bands: s – strong, m – medium, w – weak, v – very, sh – shoulder, br – broad.

corresponding authors: maciej.debowski@pw.edu.pl; piogun@ch.pw.edu.pl

Table S1. Structural details of weak π-stacking interactions between *p*-$C_6H_4NO_2$ groups leading to the formation of layers parallel to (001) lattice plains in compound **1**. Distances given in Å and angles in degrees.

Interaction	Cg···Cg	Dihedral angle	Slippage
Cg2···Cg2^{i}	4.220(7)	11.7(6)	2.257
Cg2···Cg2^{ii}	4.219(7)	11.7(6)	2.775
Cg4···Cg4^{i}	4.179(7)	10.5(6)	2.667
Cg4···Cg4^{ii}	4.180(7)	10.5(6)	2.212

Y–X···Cg interaction	X···Cg	Y···Cg	Y–X···Cg
N2–O12···Cg2^{i}	3.996(12)	3.979(12)	80.3(8)

i = −½ + *x*, ½ − *y*, *z*; ii = ½ + *x*, ½ − *y*, *z*. Ring2 = C7C8C9C10C11C12; Ring4 = C19C20C21C22C23C24

Table S2. Structural details of C–H···O hydrogen bonds in compound **1**. Distances given in Å and angles in degrees.

Interaction	H···O	C···O	C–H···O
C5–H5···O12^{i}	2.53	3.204(17)	128
C17–H17···O15^{i}	2.60	3.249(16)	126
C2–H2···O13^{iii}	2.51	3.163(16)	126
C9–H9···O14^{iv}	2.51	3.335(18)	145
C23–H23···O10^{v}	2.33	3.300(17)	151

i = −½ + *x*, ½ − *y*, *z*; iii = ½ − *x*, −½ + *y*, ½ + *z*; iv = −*x*, 1 − *y*, ½ + *z*; v =½ − *x*, −½ + *y*, −½ + *z* .

Table S3. Structural details of π-stacking interactions between *p*-$C_6H_4NO_2$ groups stiffening polymeric rods running along [100] crystallographic direction in compound **1**. Distances given in Å and angles in degrees.

Interaction	Cg···Cg	Dihedral angle	Slippage
Cg1···Cg1^{vi}	3.802(6)	11.3(5)	1.415
Cg1···Cg1^{vii}	3.801(6)	11.3(5)	1.154
Cg3···Cg3^{vi}	3.842(7)	11.1(6)	1.346
Cg3···Cg3^{vii}	3.841(7)	11.1(6)	1.675

vi = −½ + *x*, 1.5 − *y*, *z*; vii = ½ + *x*, 1.5 − *y*, *z*. Ring1 = C1C2C3C4C5C6; Ring3 = C13C14C15C16C17C18

corresponding authors: maciej.debowski@pw.edu.pl; piogun@ch.pw.edu.pl

Table S4. Selected torsion angles connected with conformation of organic substituents around phosphorus centers in compounds **1**–**3**.

Compound	Bond	Torsion angle (°)	Conformation type [a]
1	O7–P1–O8–C19	−66.3(10)	G^-
	O8–P1–O7–C13	−66.3(9)	G^-
	O3–P2–O4–C7	−68.3(10)	G^-
	O4–P2–O3–C1	−64.2(9)	G^-
2	O14–P3–O13–C29	−59.18(16)	G^-
	O13–P3–O14–C36	−73.59(14)	G^-
	O9–P1–O10–C8	59.38(14)	G^+
	O10–P1–O9–C1	60.43(12)	G^+
	O12–P2–O11–C15	65.99(12)	G^+
	O11–P2–O12–C22	54.75(12)	G^+
	O15–P4–O16–C50	172.4(4)	T
	O16–P4–O15–C43	−68.92(14)	G^-
3	O3–P1–O4–C1	−57.98(17)	G^-
	O4–P1–O3–C11	−64.26(17)	G^-
	O8–P2–O7–C21	−66.45(15)	G^-
	O7–P2–O8–C31	154.73(16)	T

[a] symbol of the conformational arrangement in accordance with IUPAC recommendations.[1]

References

1. IUPAC Compendium of Chemical Terminology (the "Gold Book"), https://goldbook.iupac.org/terms/view/T06406, (accessed January 2022).

corresponding authors: maciej.debowski@pw.edu.pl; piogun@ch.pw.edu.pl

Calculations of bond–valence vectors for zinc and phosphorus centers in compounds 1–3

Bond valences were calculated using the most widely used equation describing the relationship between the bond length (d_{ij}) between the i–th and j–th atoms and the valence of this bond (s_{ij}):[1]

$$s_{ij} = \exp\left[\left(r_{ij} - d_{ij}\right) \times b^{-1}\right] \quad \text{(S1)}$$

where r_{ij} and b are empirically determined constants for the given i–j bond. r_{ij} is equal to the length of a conceptual bond of a unit valence, whereas the parameter b is generally treated as a 'universal' constant, often taken to be 0.37 Å.[1,2] The following parameters were used in the calculations: r_{PO}= 1.617 Å (b = 0.37 Å),[3] and r_{ZnO} = 1.704 Å (b = 0.37 Å),[3] together with the experimental d_{ij} values derived from a single–crystal X–ray analysis of compounds 1–3.

According to the bond–valence vector model,[4] the bond between the coordination center i and the more electronegative ligating atom j of s_{ij} valence can be represented by the bond–valence vector v_{ij} directed from i to j with a length defined by the following equation:

$$\left|\mathbf{v}_{ij}\right| = s_{ij} \times \left[1 - \left(s_{ij} \times Q_i^{-1}\right)\right] \text{ (S2)}$$

where Q_i is the charge in the core of the central i–th atom. The lengths of the individual bond–valence vectors ($|v_{ZnO}|$ and $|v_{PO}|$) were calculated by setting the zinc core charge Q_{Zn}= 2 and the phosphorus core charge Q_P= 5.

The bond–valence sums (S_i) and lengths of the resultant bond–valence vectors ($|v_i|$) for each coordination centers i connected to the ligating oxygen atoms j were calculated according to the following equations:

$$S_i = \sum_j s_{ij} \quad \text{(S3)}$$

$$\mathbf{v}_i = \sum_j \mathbf{v}_{ij} \quad \text{(S4)}$$

$$|\mathbf{v}_i| = (\mathbf{v}_i \cdot \mathbf{v}_i)^{0.5} \quad \text{(S5)}$$

Table S5. Bond–valence sum (S_i) and length of the resultant bond–valence vector $|v_i|$ for each crystallographically independent zinc or phosphorus coordination center in compounds 1–3 and zinc bis(diphenylphosphate) (**ZnDPhP**)

Compound	Atom	S_P	$\|\mathbf{v}_P\|$ (v.u.)[a]	Atom	S_{Zn}	$\|\mathbf{v}_{Zn}\|$ (v.u.)[a]
1	P1	4.88	0.033	Zn1	2.08	0.074
	P2	4.98	0.026			
2	P1	5.03	0.010	Zn1	2.18	0.029
	P2	5.03	0.042	Zn2	2.17	0.041
	P3	5.05	0.024			
	P4	5.05	0.075			
3	P1	5.10	0.030	Zn1	2.24	0.056
	P2	5.07	0.051			
ZnDPhP[b]	P1	5.02	0.062	Zn1	2.18	0.034
	P2	4.97	0.057			

[a] valence units. [b] data from reference 5

References

1. I. D. Brown and D. Altermatt, *Acta Crystallogr., Sect. B: Struct. Sci.,* 1985, **41**, 244–247.
2. N. E. Brese and M. O'Keeffe, *Acta Crystallogr., Sect. B: Struct. Sci.*, 1991, **47**, 192–197.

corresponding authors: maciej.debowski@pw.edu.pl; piogun@ch.pw.edu.pl

3. I D. Brown, Accumulated Table of Bond Valence Parameters, https://www.iucr.org/__data/assets/file/0011/150779/bvparm2020.cif (accessed Dec 6, 2019) .
4. J. Zachara, *Inorg. Chem.*, 2007, **46**, 9760–9767.
5. M. Dębowski, Z. Florjańczyk, A. Ostrowski, P. A. Guńka, J. Zachara, A. Krztoń–Maziopa, J. Chazarkiewicz, A. Iuliano and A. Plichta, *RSC Adv.*, 2021, **11**, 7873–7885.

Table S6. Thermogravimetric data of compounds **1**–**3** measured in argon

Compound	Type of process[a]	Degradation step, n[b]	$T_{b,n}$[c] (°C)	$T_{98\%}$[d] (°C)	$T_{95\%}$[d] (°C)	$T_{onset,n}$[e] (°C)	$T_{max,n}$[f] (°C)	$T_{endset,n}$[e] (°C)	Δm[g] (wt%)	m_{800}[h] (wt%)
1	one–step	1	274.0	326.5	363.1	382.4	382.5	382.7	51.55	40.45
2	multistep	1	288.0	337.9	357.1	355.3	369.3	556.1[i]	44.63	51.88
3	two–step	1	264.0	283.5	302.2	316.4	324.4	327.3	35.28	41.79
		2	449.0	–	–	485.1	501.3	522.6	14.24	

[a] Refers to the number of steps in which thermal decomposition occurred, *e.g.* two–step – two well–separated steps of weight loss, multistep – many steps of weight loss, some overlapping with each other. [b] An individual number ascribed to the respective decomposition region. [c] Temperature of the beginning of weight loss (a bend point on the TG curve for the respective decomposition region denoted with its individual index n). [d] $T_{98\%}$ and $T_{95\%}$ denote temperatures at which sample mass reached 98% and 95% of its initial value, respectively. [e] $T_{onset,n}$ and $T_{endset,n}$ denote the extrapolated onset and endset temperatures, respectively. [f] $T_{max,n}$ – temperature at the maximum decomposition rate for the respective decomposition step. [g] Mass variation during the respective decomposition step (as % of the initial sample mass). [h] Residual mass of the sample measured at 800 °C (as % of the initial sample mass).

corresponding authors: maciej.debowski@pw.edu.pl; piogun@ch.pw.edu.pl

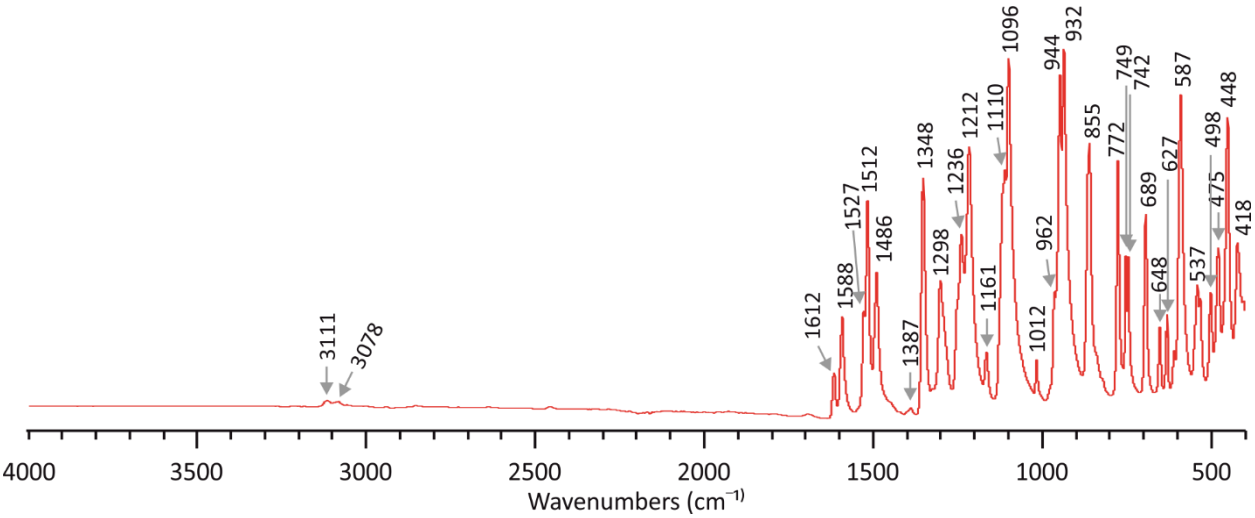

Figure S1. FTIR spectrum of compund **1**.

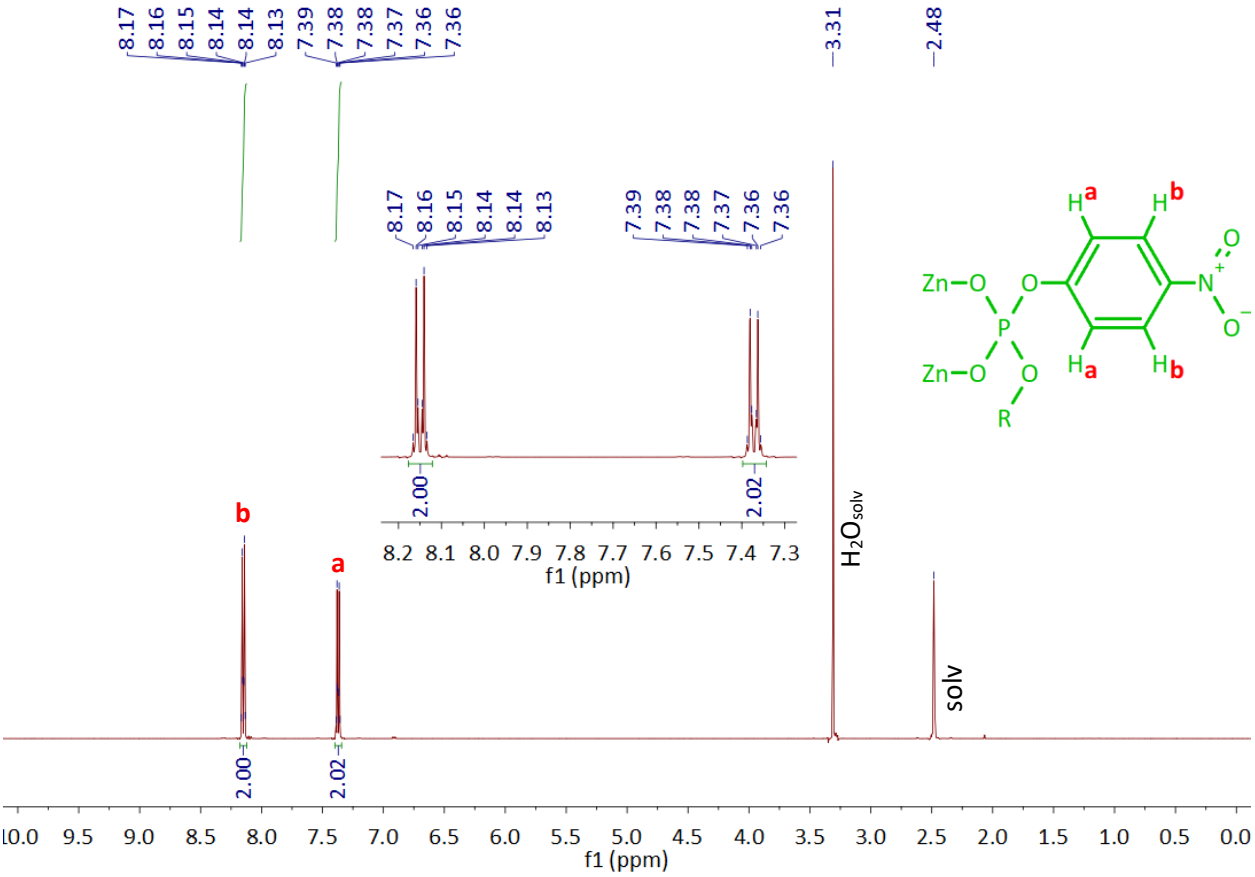

Figure S2. [1]H NMR spectrum of compound **1** recorded at room temperature. Sample dissolved in DMSO-d_6. Abbreviations: **H_2O_{solv}** – traces of water present in DMSO-d_6, **solv** – solvent residual signal.

[1]H NMR (500 MHz; DMSO-d_6; residual solvent) δ_H 8.18–8.12 (2 H, m, 3-H and 5-H), 7.40–7.34 (2 H, m, 2-H and 6-H).

corresponding authors: maciej.debowski@pw.edu.pl; piogun@ch.pw.edu.pl

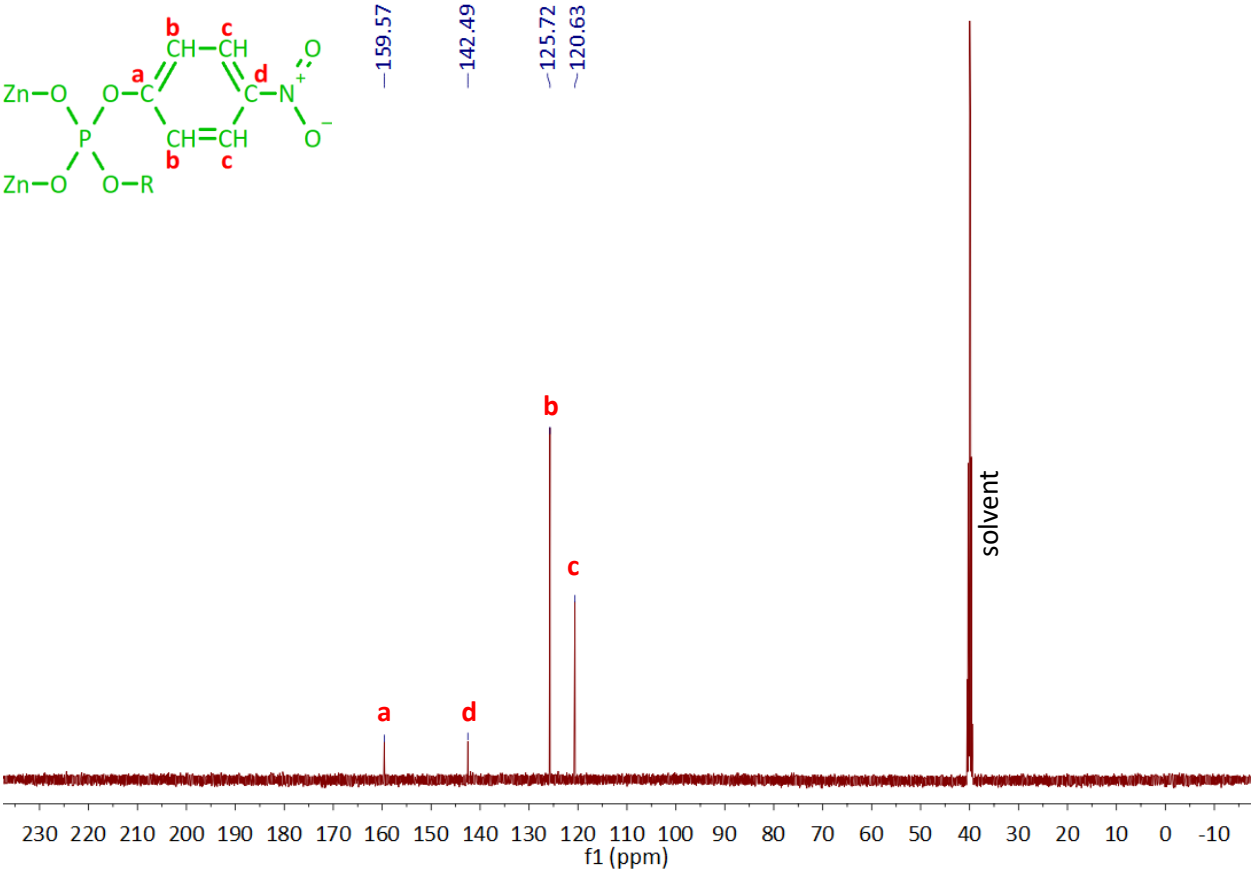

Figure S3. ^{13}C NMR spectrum of compound **1** recorded at room temperature. Sample dissolved in DMSO-d_6. Solvent residual signal is also indicated.

^{13}C NMR (126 MHz; DMSO-d_6; residual solvent) δ_C 159.57, 142.49, 125.72, 120.63.

corresponding authors: maciej.debowski@pw.edu.pl; piogun@ch.pw.edu.pl

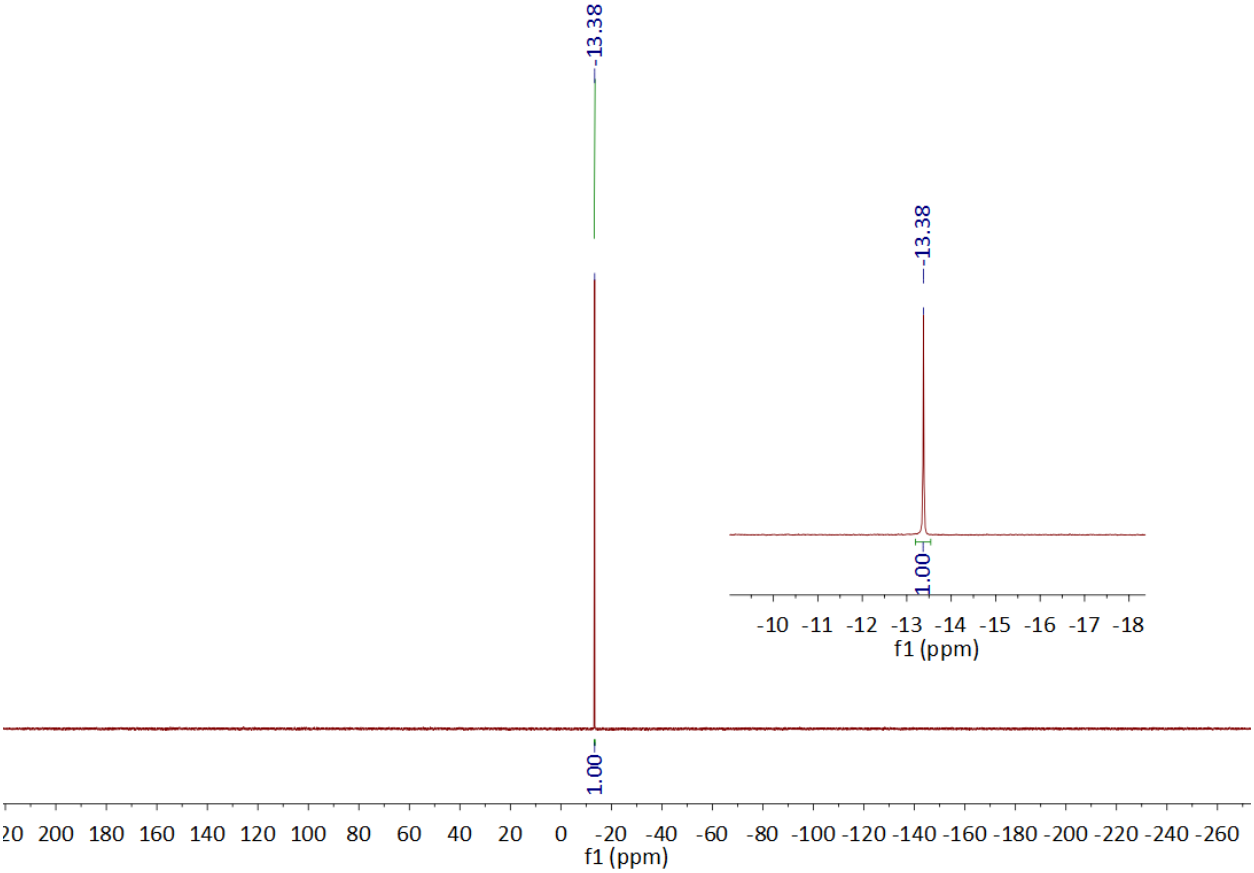

Figure S4. ^{31}P NMR spectrum of compound **1** recorded at room temperature. Sample dissolved in DMSO-d_6. The chemical shifts are reported relative to 85% H_3PO_4 external standard.

^{31}P NMR (202 MHz; DMSO-d_6; 85% H_3PO_4) δ_P −13.38.

corresponding authors: maciej.debowski@pw.edu.pl; piogun@ch.pw.edu.pl

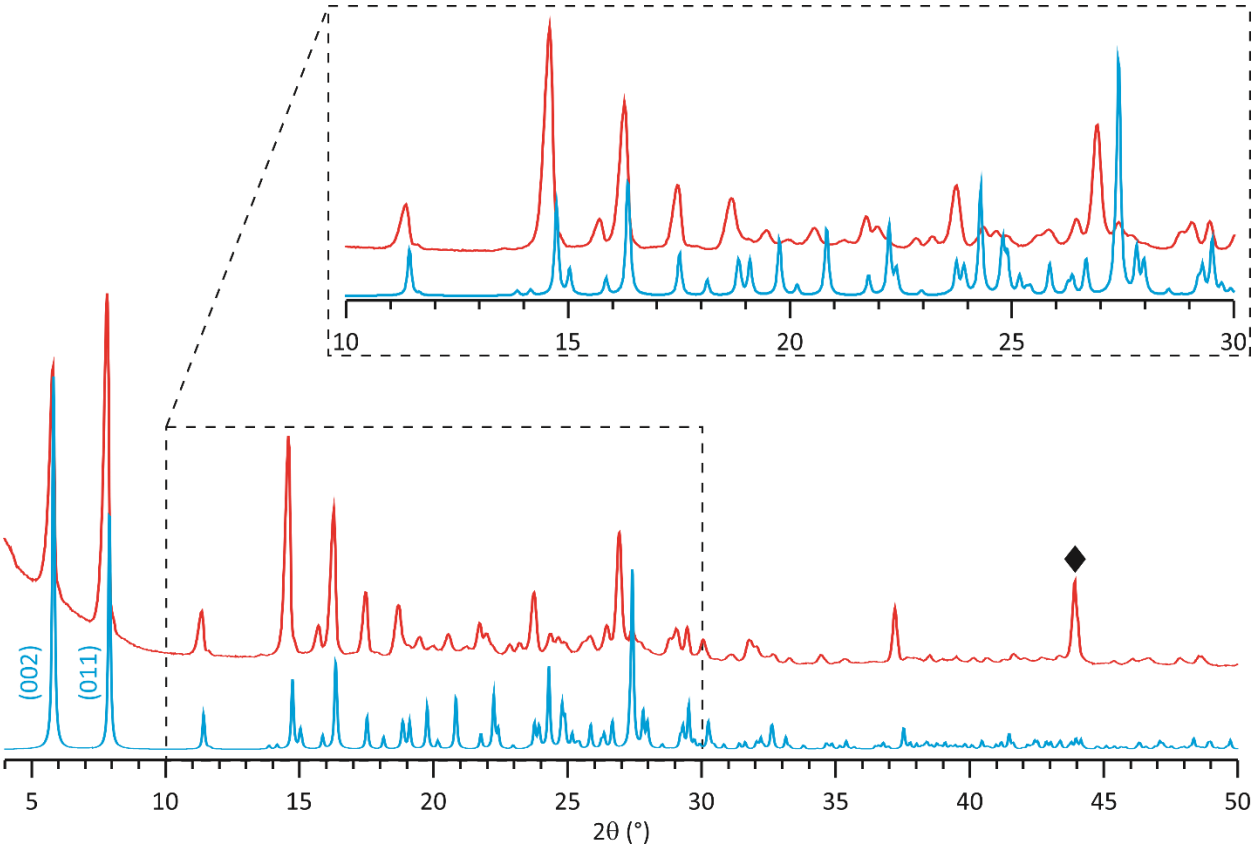

Figure S5. The experimental PXRD pattern of compound **1** recorded at room temperature (—) and PXRD pattern simulated from a single–crystal X–ray measurement carried out at 100 K (—). The reflection observed for a polycrystalline sample around 44° (denoted with ♦) results from diamond powder used as an internal standard. Miller indices of two major reflections are denoted. The diffractograms are normalized between 0 and 1.

corresponding authors: maciej.debowski@pw.edu.pl; piogun@ch.pw.edu.pl

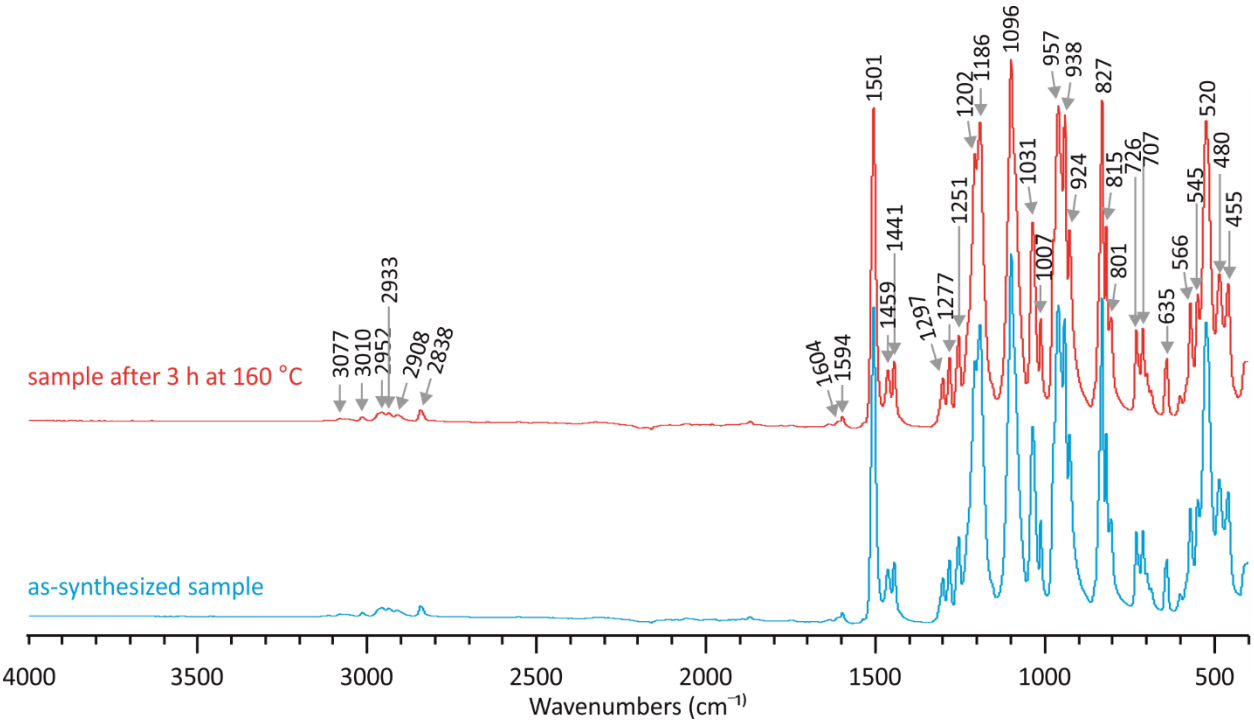

Figure S6. FTIR spectra of compound **2** recorded at room temperature: before thermal treatment (—) and after conditioning at 160 °C for 3 h (—).

corresponding authors: maciej.debowski@pw.edu.pl; piogun@ch.pw.edu.pl

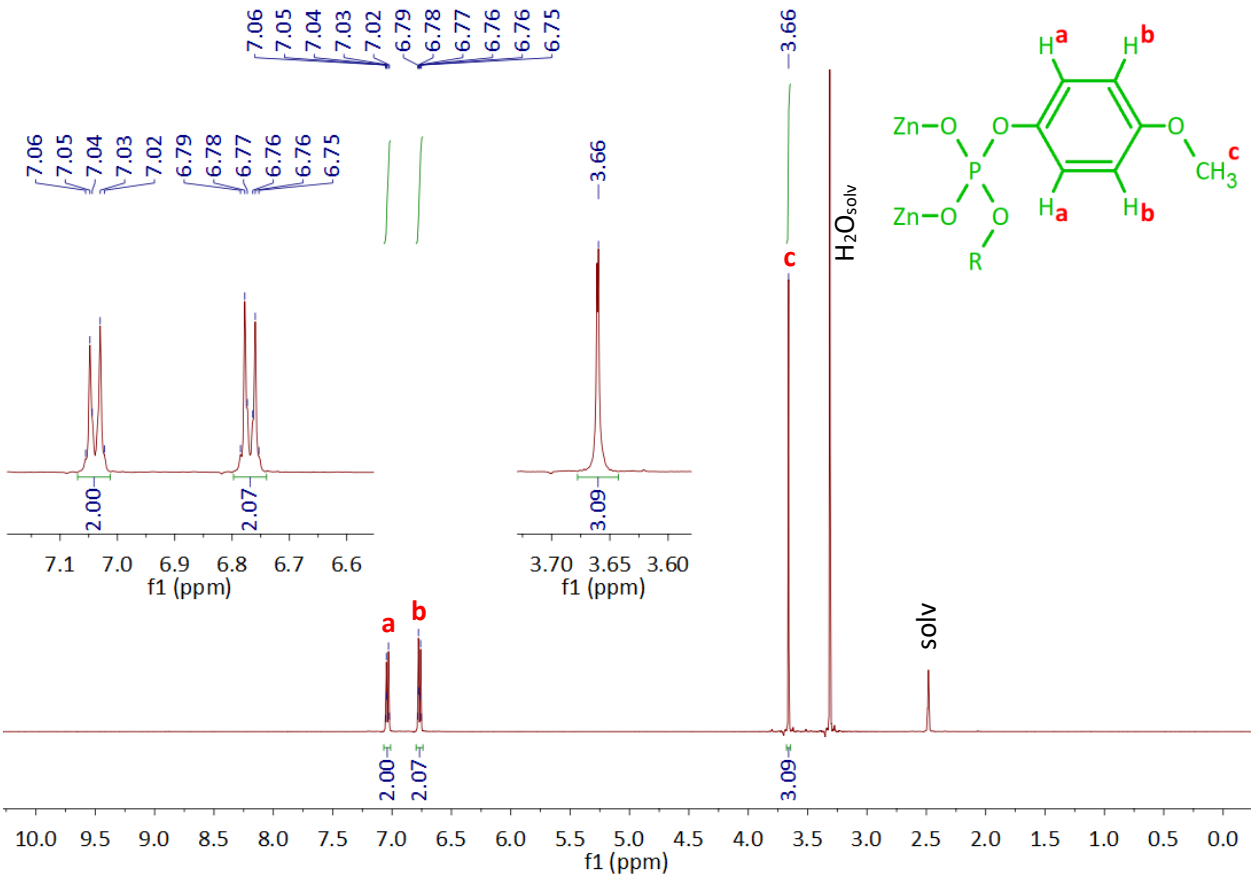

Figure S7. ^{1}H NMR spectrum of compound **2** recorded at room temperature. Sample dissolved in DMSO-d_6. Abbreviations: **H_2O_{solv}** – traces of water present in DMSO-d_6, **solv** – solvent residual signal.

^{1}H NMR (500 MHz; DMSO-d_6; residual solvent) δ_H 7.07–7.01 (2 H, m, 2-H and 6-H),6.80–6.74 (2 H, m, 3-H and 5-H), 3.66 (3H, s, OCH_3).

corresponding authors: maciej.debowski@pw.edu.pl; piogun@ch.pw.edu.pl

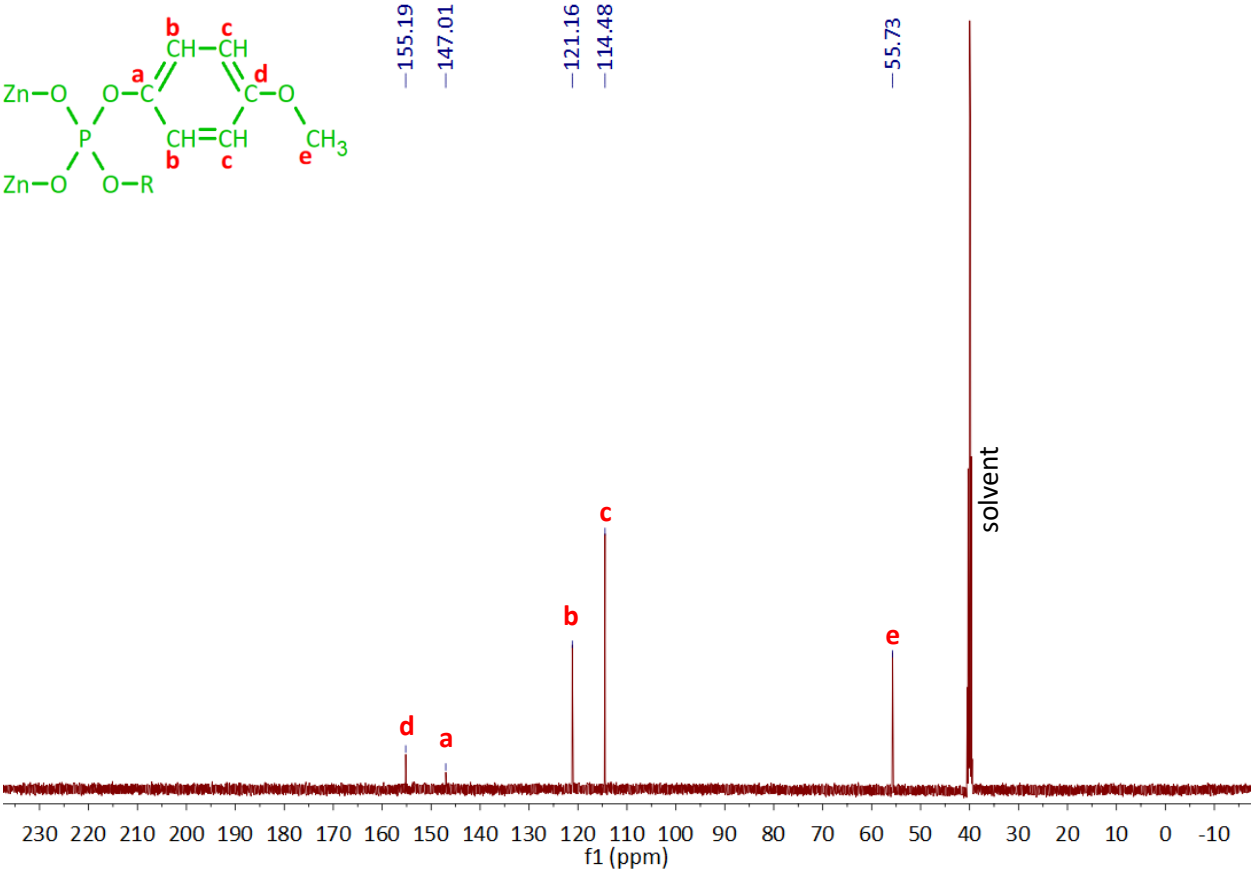

Figure S8. ^{13}C NMR spectrum of compound **2** recorded at room temperature. Sample dissolved in DMSO-d_6. Solvent residual signal is also indicated.

^{13}C NMR (126 MHz; DMSO-d_6; residual solvent) δ_C 155.19, 147.01, 121.16, 114.48, 55.73.

corresponding authors: maciej.debowski@pw.edu.pl; piogun@ch.pw.edu.pl

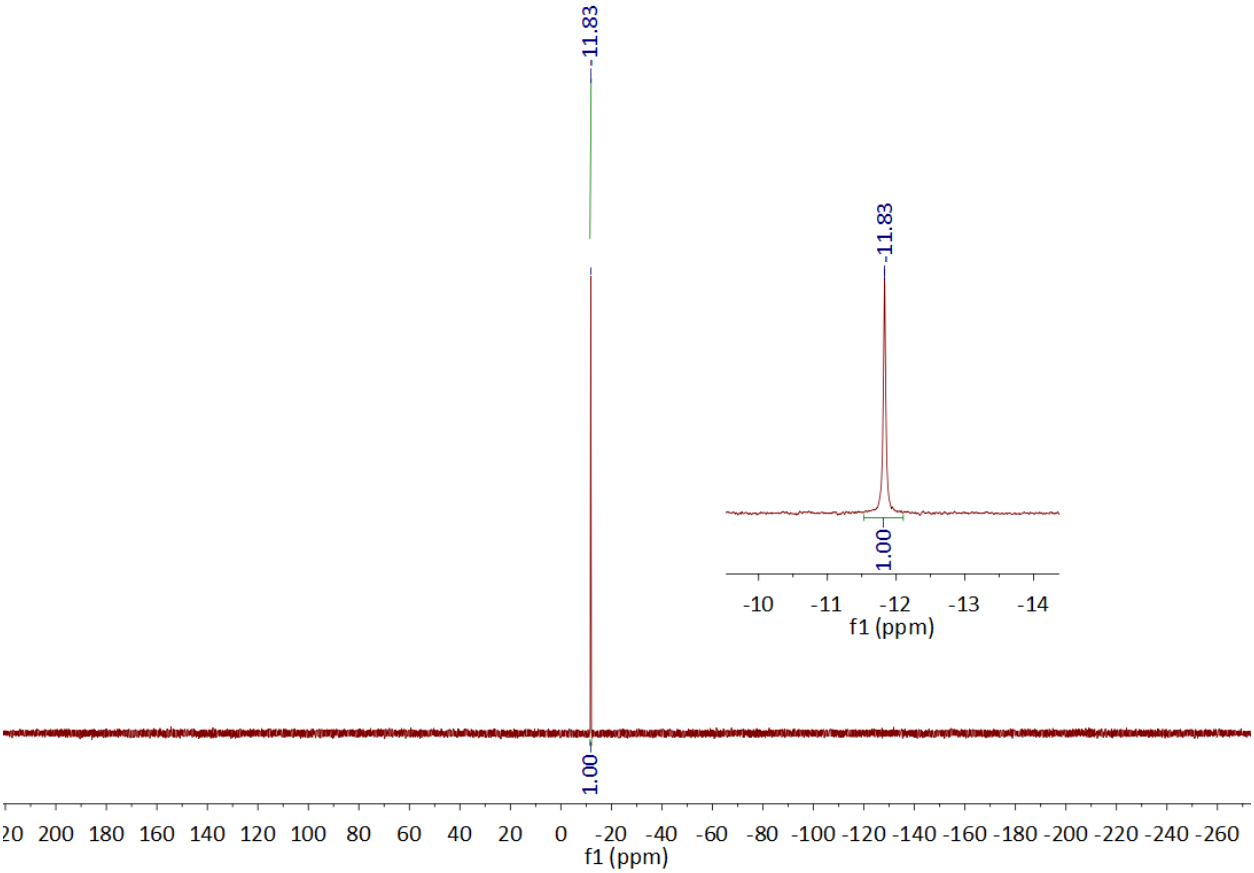

Figure S9. ^{31}P NMR spectrum of compound **2** recorded at room temperature. Sample dissolved in DMSO-d_6. The chemical shifts are reported relative to 85% H_3PO_4 external standard.

^{31}P NMR (202 MHz; DMSO-d_6; 85% H_3PO_4) δ_P −11.83.

corresponding authors: maciej.debowski@pw.edu.pl; piogun@ch.pw.edu.pl

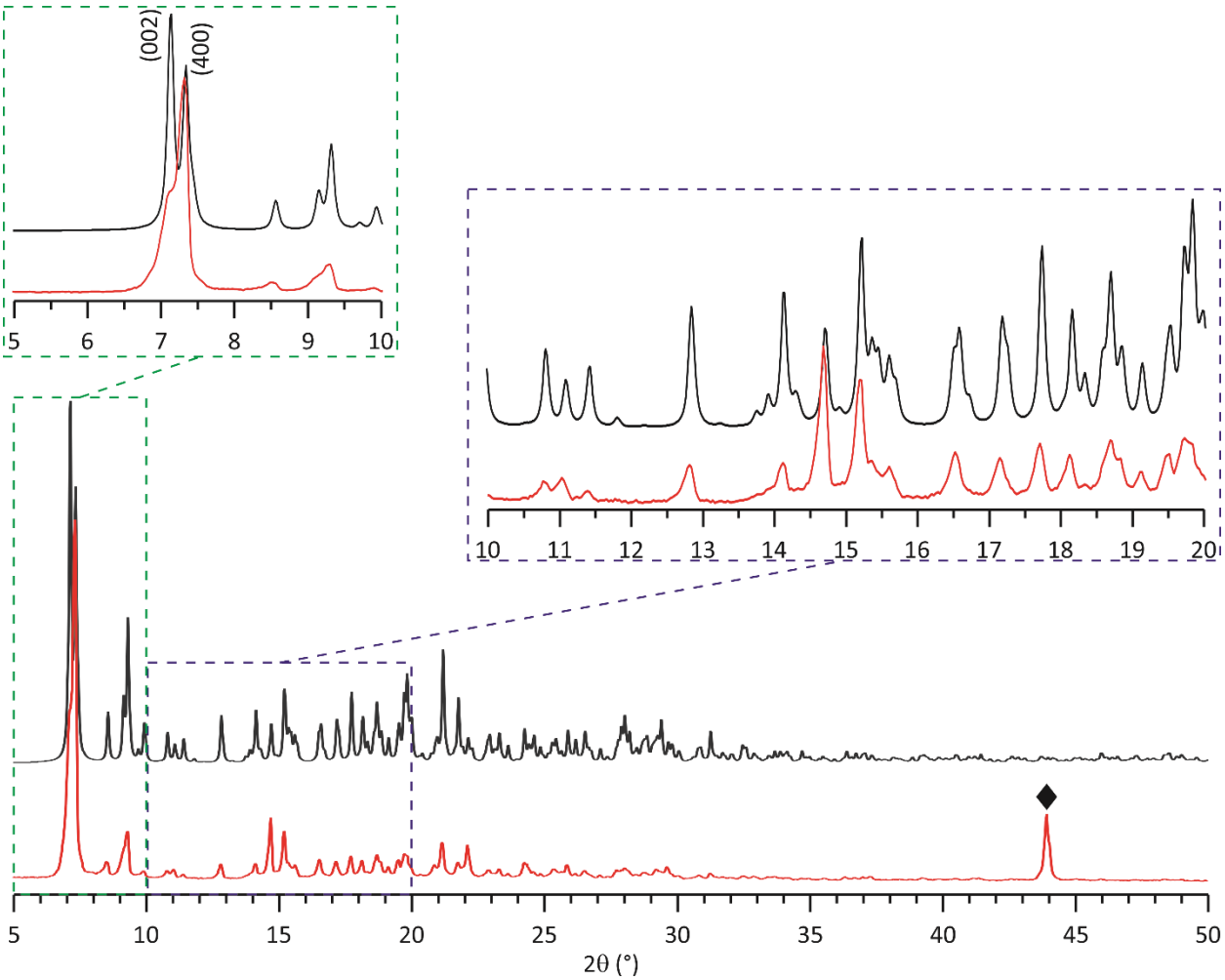

Figure S10. The experimental PXRD pattern of compound **2** recorded at room temperature (—) and PXRD pattern simulated from a single–crystal X–ray measurement (—). The reflection observed for a polycrystalline sample around 44° (denoted with ♦) results from diamond powder used as an internal standard. Miller indices of two major reflections are denoted. The diffractograms are normalized between 0 and 1.

corresponding authors: maciej.debowski@pw.edu.pl; piogun@ch.pw.edu.pl

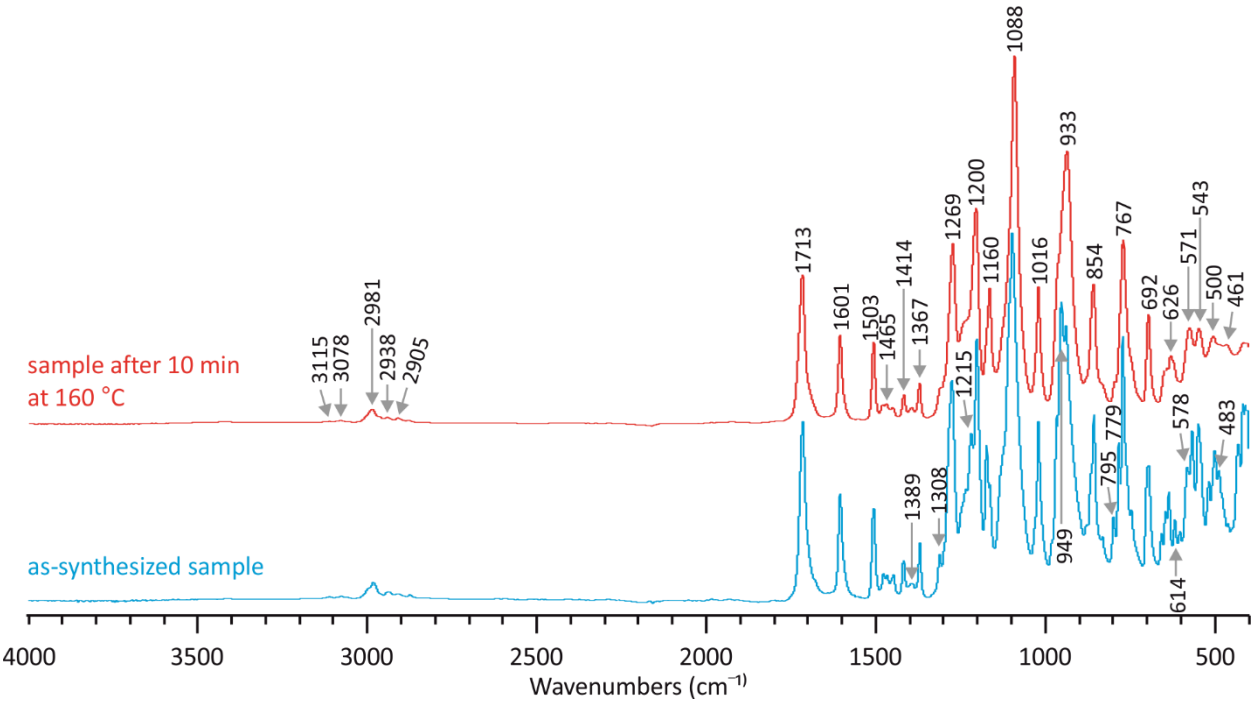

Figure S11. FTIR spectra of compound **3** recorded at room temperature: before thermal treatment (—) and after conditioning at 160 °C for 10 minutes (—).

corresponding authors: maciej.debowski@pw.edu.pl; piogun@ch.pw.edu.pl

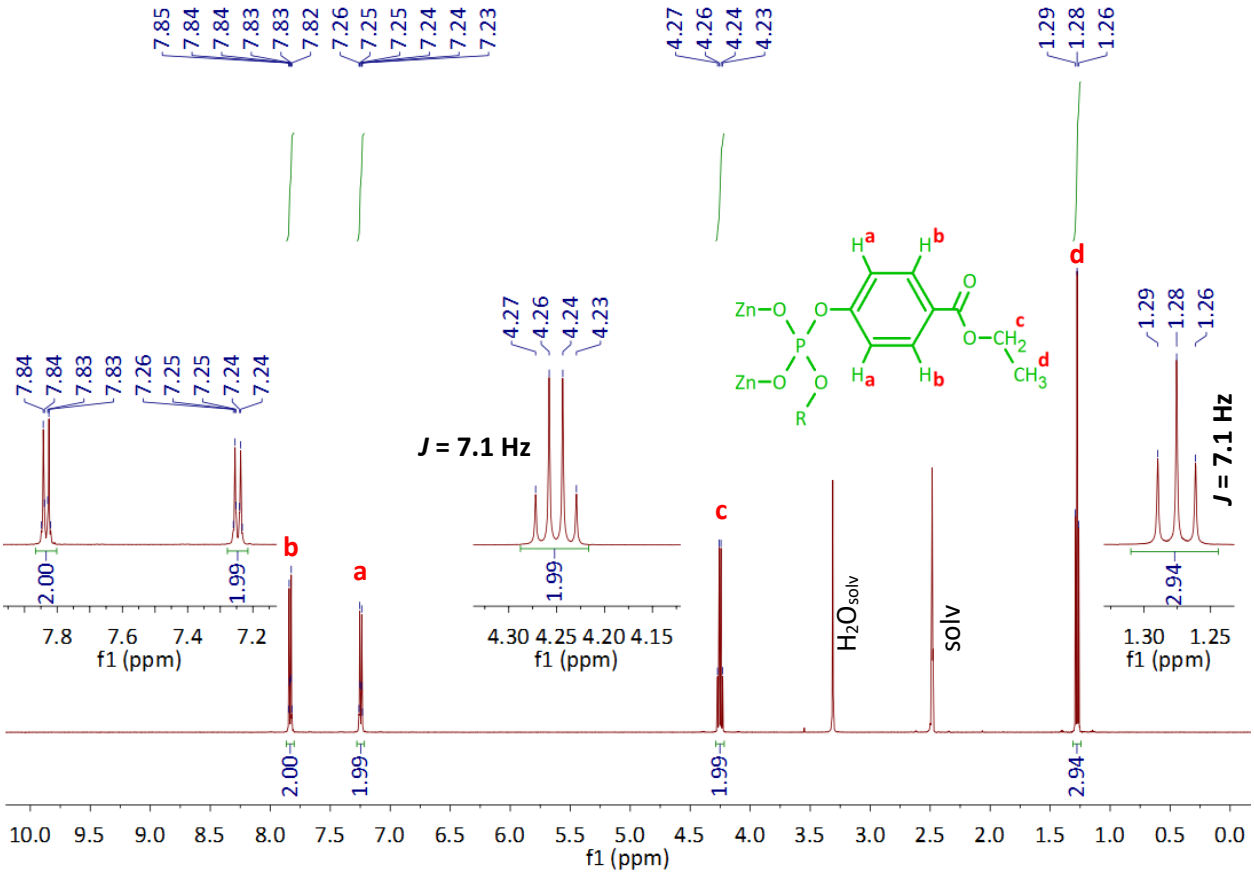

Figure S12. ^{1}H NMR spectrum of compound **3** recorded at room temperature. Sample dissolved in DMSO-d_6. Abbreviations: **H_2O_{solv}** – traces of water present in DMSO-d_6, **solv** – solvent residual signal.

^{1}H NMR (500 MHz; DMSO-d_6; residual solvent) δ_H 7.87–7.80 (2 H, m, 3-H and 5-H), 7.28–7.22 (2 H, m, 2-H and 6-H), 4.25 (2 H, q, J = 7.1 Hz, CH_2CH$_3$), 1.28 (3 H, t, J = 7.1 Hz, CH$_2$CH_3)

corresponding authors: maciej.debowski@pw.edu.pl; piogun@ch.pw.edu.pl

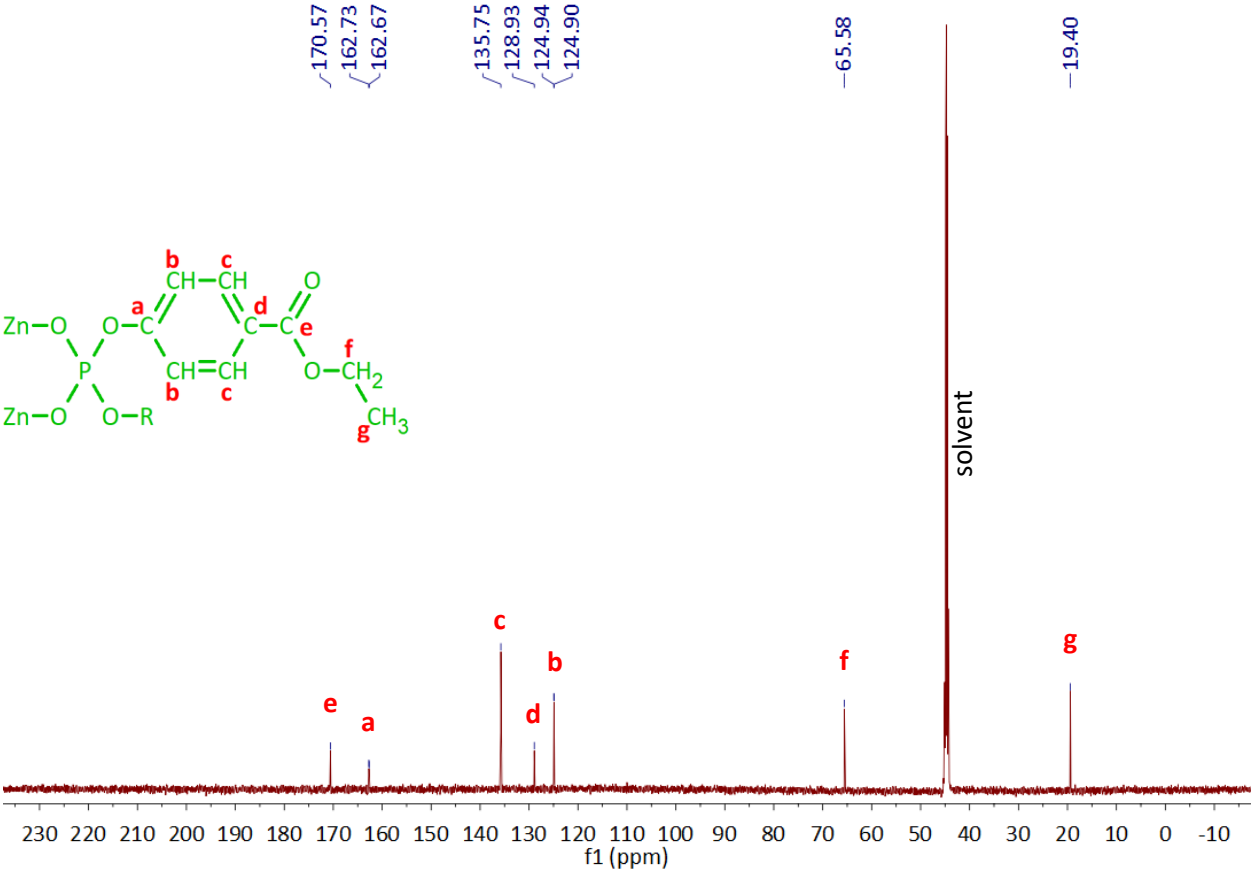

Figure S13. ^{13}C NMR spectrum of compound **3** recorded at room temperature. Sample dissolved in DMSO-d_6. Solvent residual signal is also indicated.

^{13}C NMR (126 MHz; DMSO-d_6; residual solvent) δ_C 170.57, 162.70 (d, J = 6.6 Hz), 135.75, 128.93, 124.94, 124.90, 65.58, 19.40.

corresponding authors: maciej.debowski@pw.edu.pl; piogun@ch.pw.edu.pl

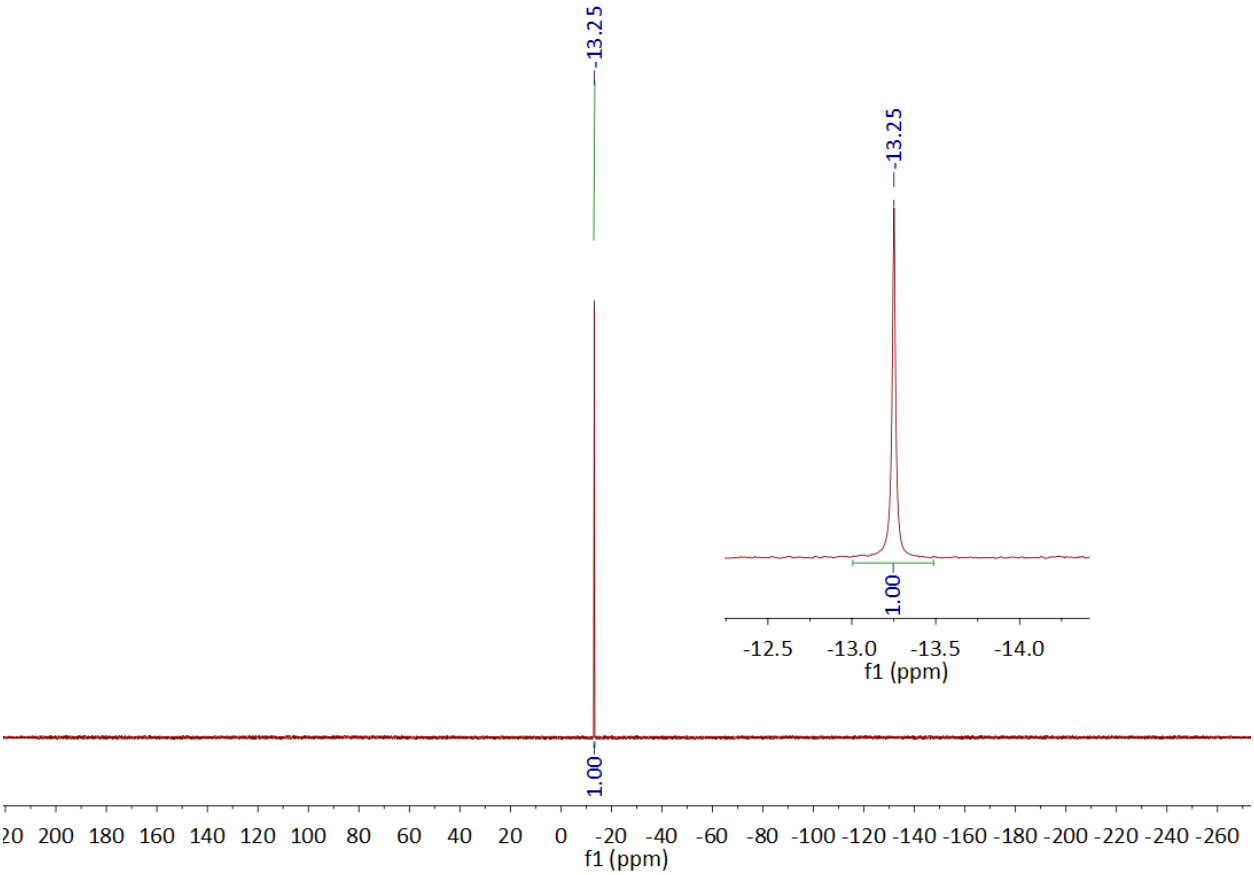

Figure S14. ^{31}P NMR spectrum of compound **3** recorded at room temperature. Sample dissolved in DMSO-d_6. The chemical shifts are reported relative to 85% H_3PO_4 external standard.

^{31}P NMR (202 MHz; DMSO-d_6; 85% H_3PO_4) δ_P −13.25.

corresponding authors: maciej.debowski@pw.edu.pl; piogun@ch.pw.edu.pl

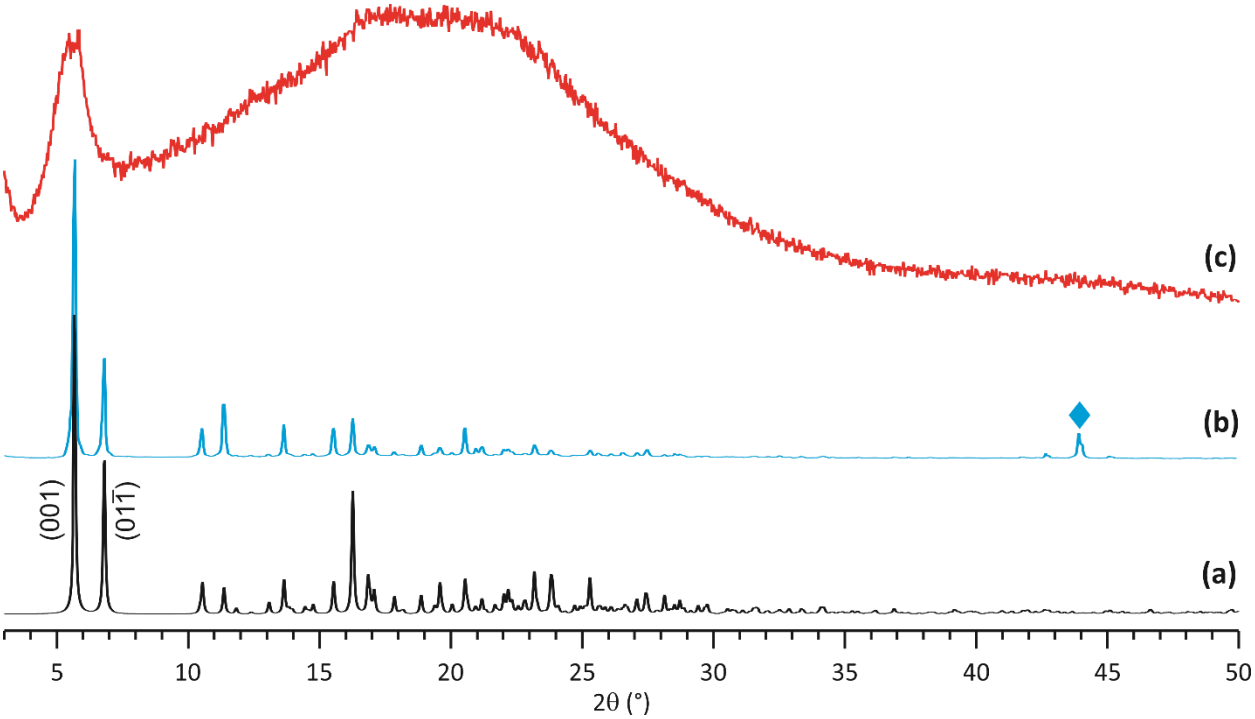

Figure S15. The simulated (**a**, —) and experimental PXRD patterns of compound **3** recorded at room temperature: before (**b**, —), and after 10 minutes of conditioning at 160 °C (**c**, —). The reflection around 44° (denoted with ♦) results from diamond powder used as an internal standard. Miller indices of two major reflections are denoted. The diffractograms were normalized between 0 and 1.

corresponding authors: maciej.debowski@pw.edu.pl; piogun@ch.pw.edu.pl

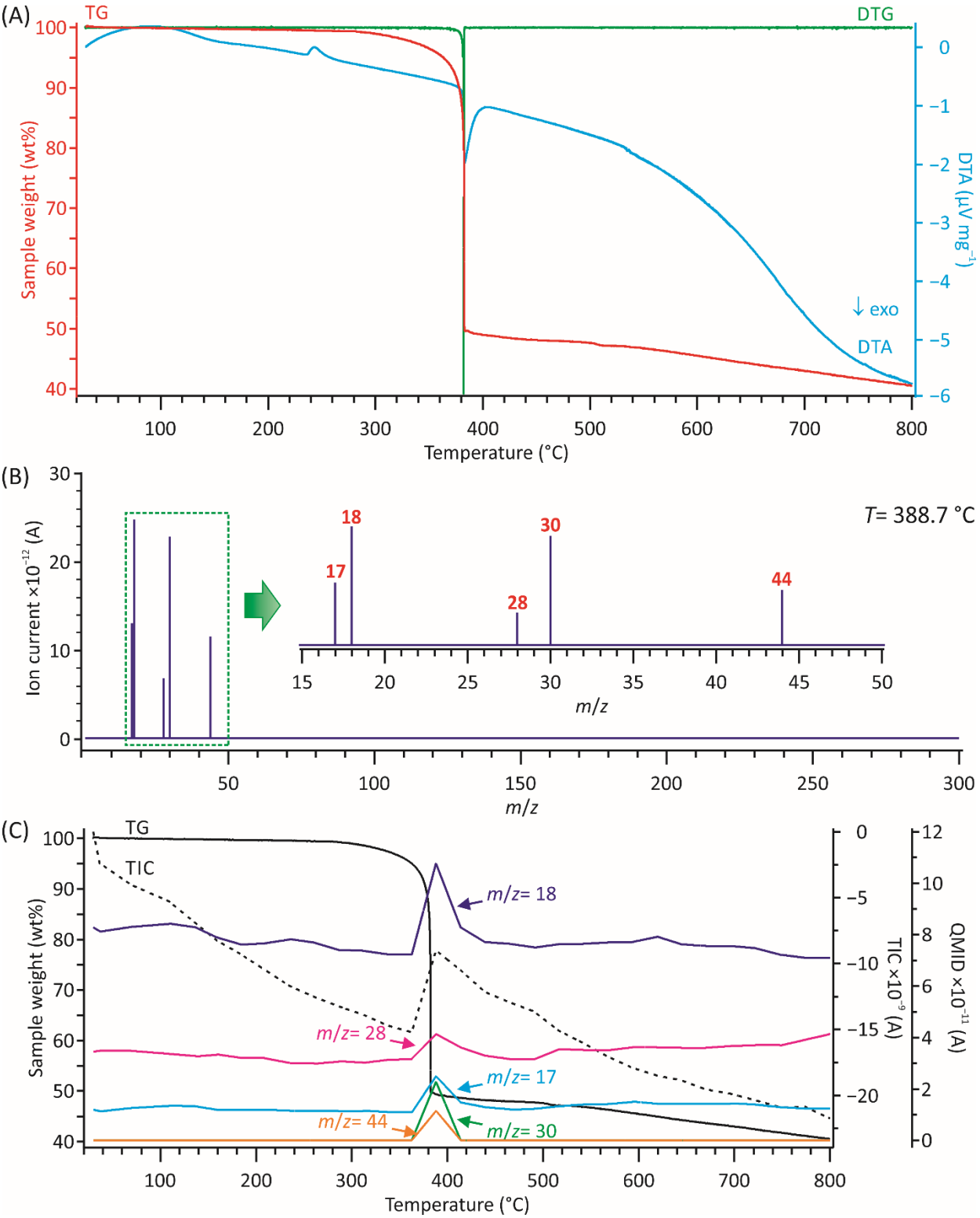

Figure S16. Simultaneous thermal analysis (STA) of compound **1** in argon (heating rate 5 °C min^{-1}) coupled with quadrupole mass spectrometry (QMS) of the evolved gases: (A) TG (—), 1st derivative of TG (DTG, —) and DTA (—) curves, (B) QMS spectrum obtained at 388.7 °C, (C) TG (—), Total Ion Current (TIC, black, dashed line) and QMS curves (coloured lines) for the ions with selected values of *m*/*z*.

corresponding authors: maciej.debowski@pw.edu.pl; piogun@ch.pw.edu.pl

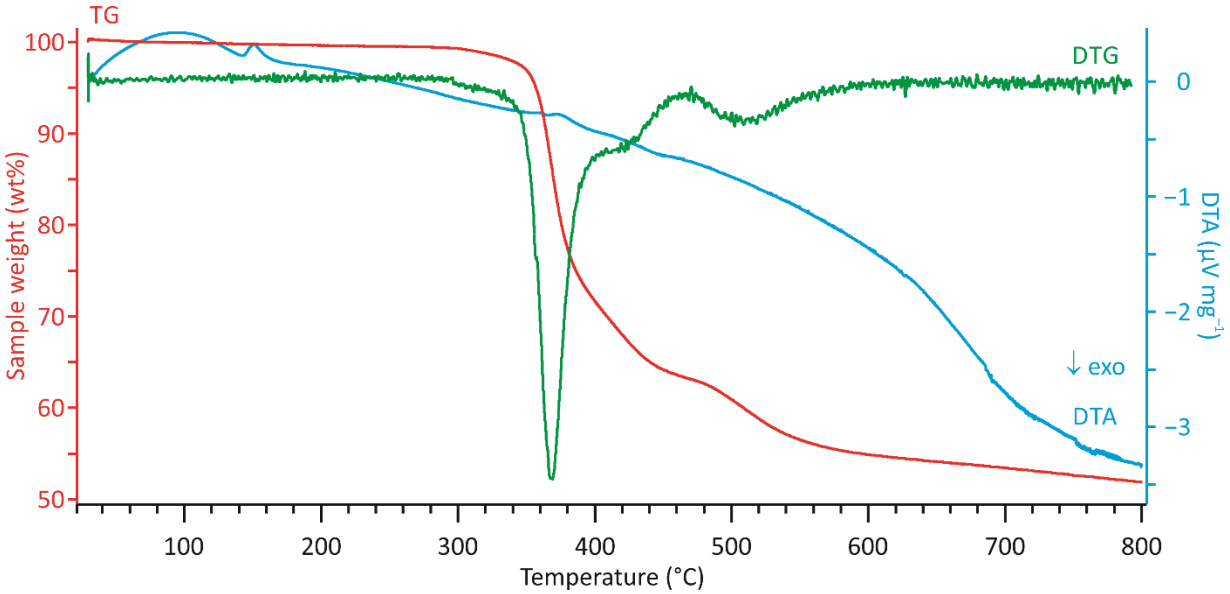

Figure S17. Simultaneous thermal analysis (STA) of compound **2** in argon (heating rate 5 °C min^{-1}): TG curve (—), 1st derivative of TG curve (DTG, —), and DTA curve (—).

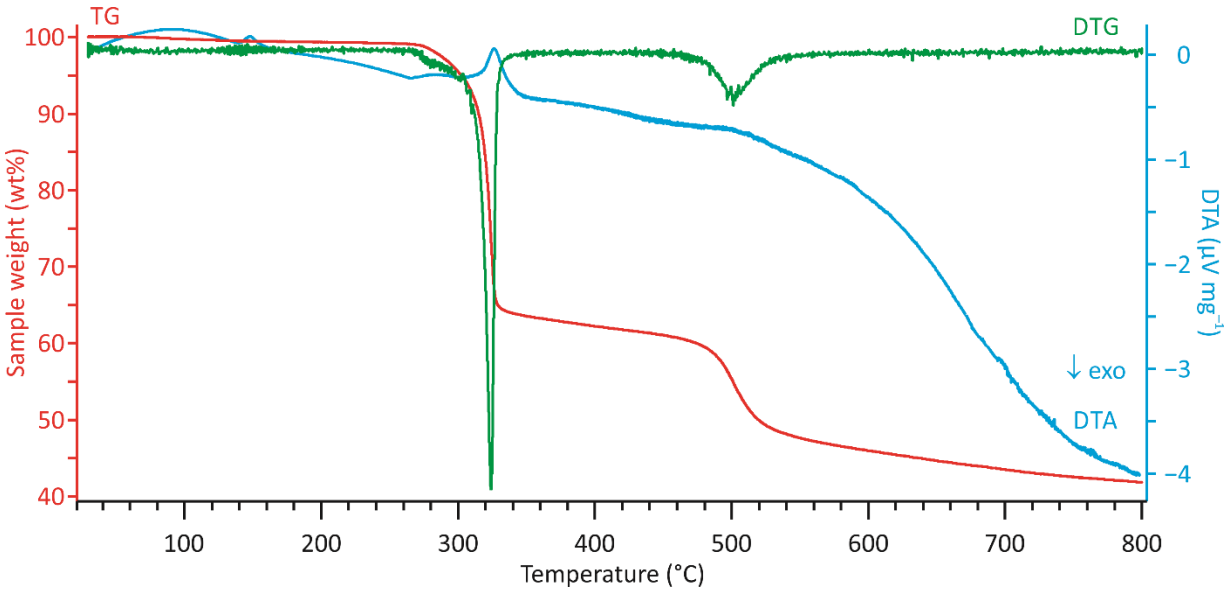

Figure S18. Simultaneous thermal analysis (STA) of compound **3** in argon (heating rate 5 °C min^{-1}): TG curve (—), 1st derivative of TG curve (DTG, —), and DTA curve (—).

corresponding authors: maciej.debowski@pw.edu.pl; piogun@ch.pw.edu.pl

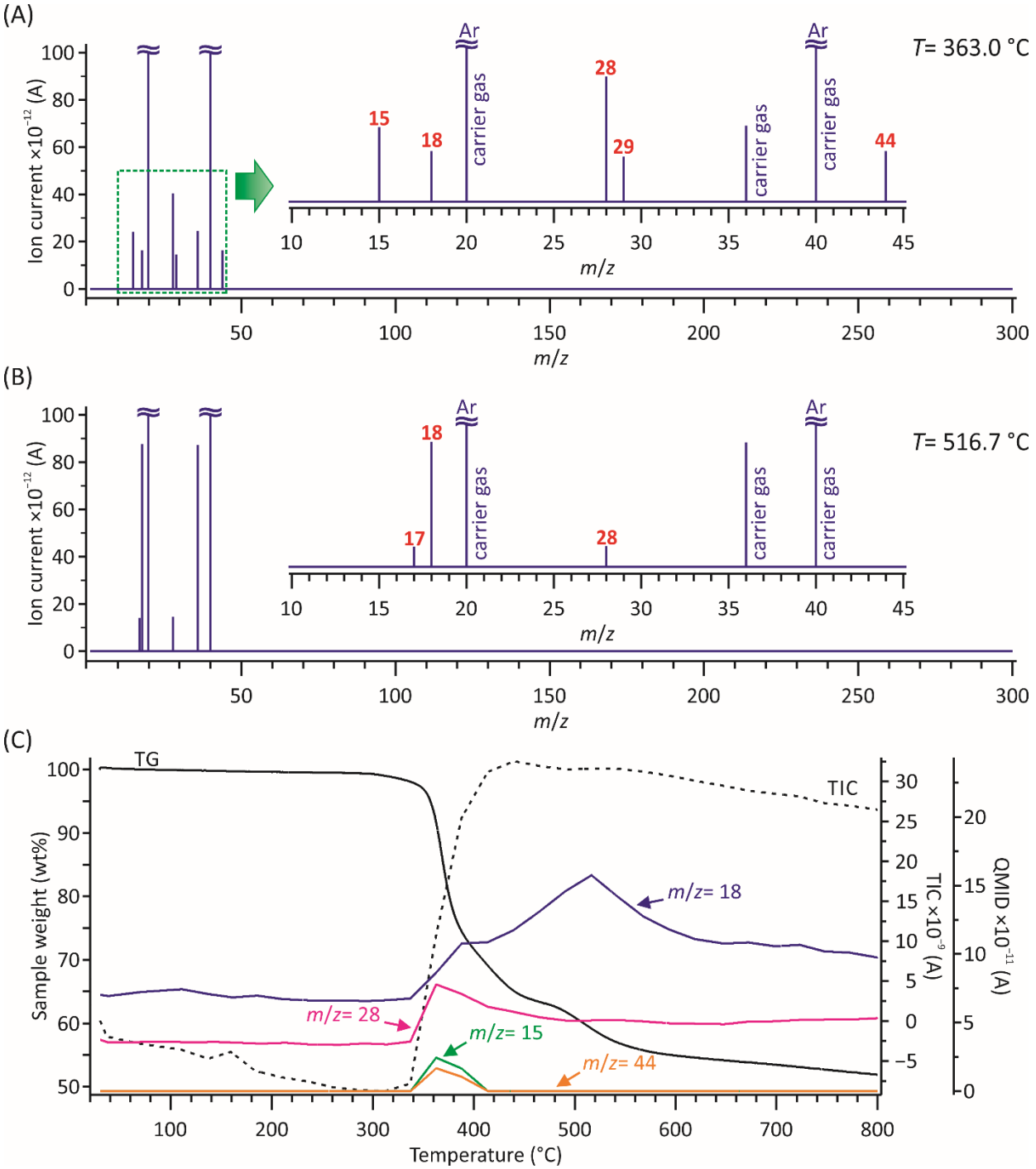

Figure S19. Simultaneous thermal analysis (STA) of compound **2** in argon (heating rate 5 °C min^{-1}) coupled with quadrupole mass spectrometry (QMS) of the evolved gases: (A) QMS spectrum obtained at 363.0 °C, (B) QMS spectrum obtained at 516.7 °C, (C) TG (black, solid line), Total Ion Current (TIC, black, dashed line) and QMS curves (coloured lines) for the ions with selected values of *m/z*.

corresponding authors: maciej.debowski@pw.edu.pl; piogun@ch.pw.edu.pl

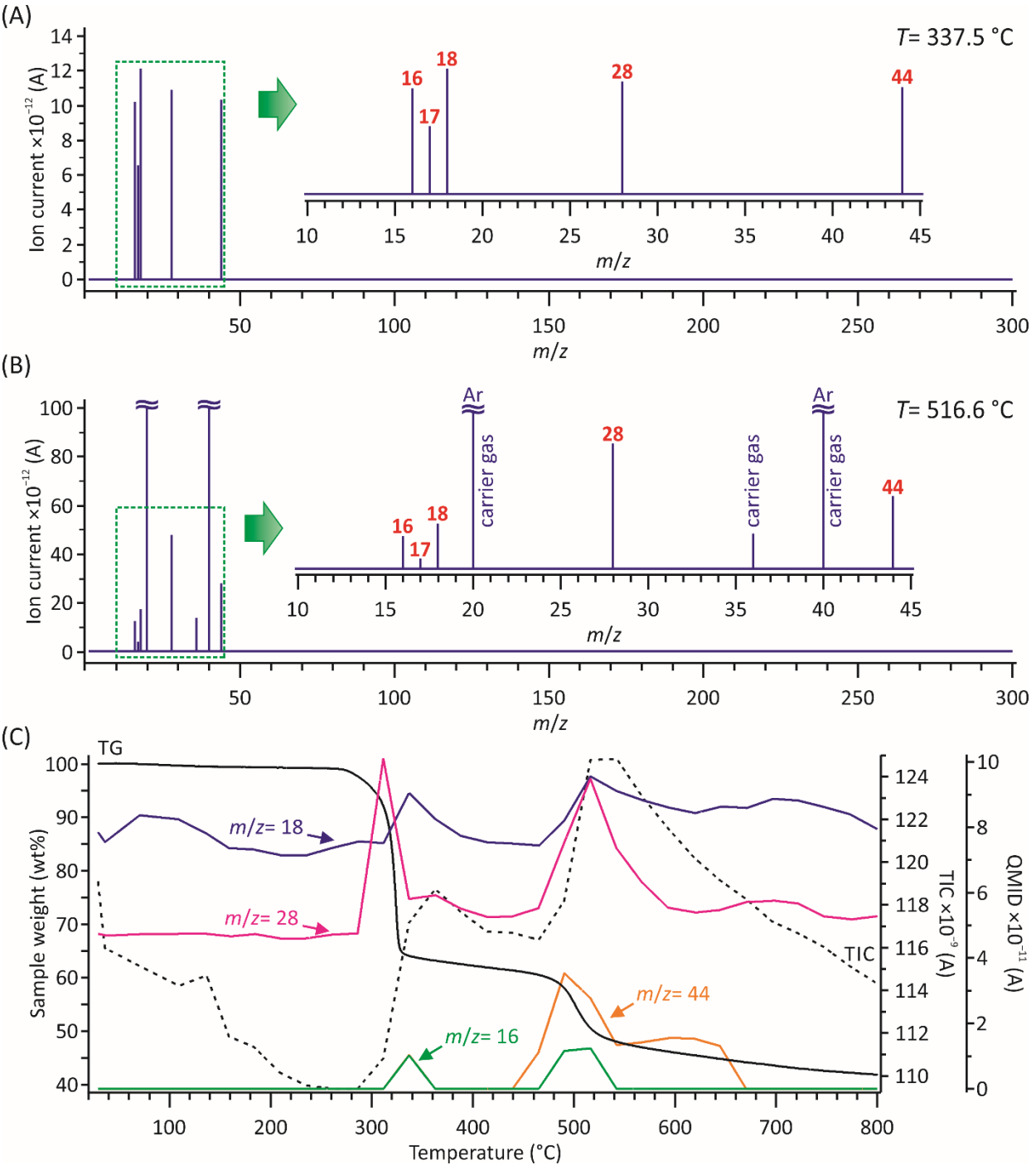

Figure S20. Simultaneous thermal analysis (STA) of compound **3** in argon (heating rate 5 °C min^{-1}) coupled with quadrupole mass spectrometry (QMS) of the evolved gases: (A) QMS spectrum obtained at 337.5 °C, (B) QMS spectrum obtained at 516.6 °C, (C) TG (black, solid line), Total Ion Current (TIC, black, dashed line) and QMS curves (coloured lines) for the ions with selected values of *m/z*.

corresponding authors: maciej.debowski@pw.edu.pl; piogun@ch.pw.edu.pl

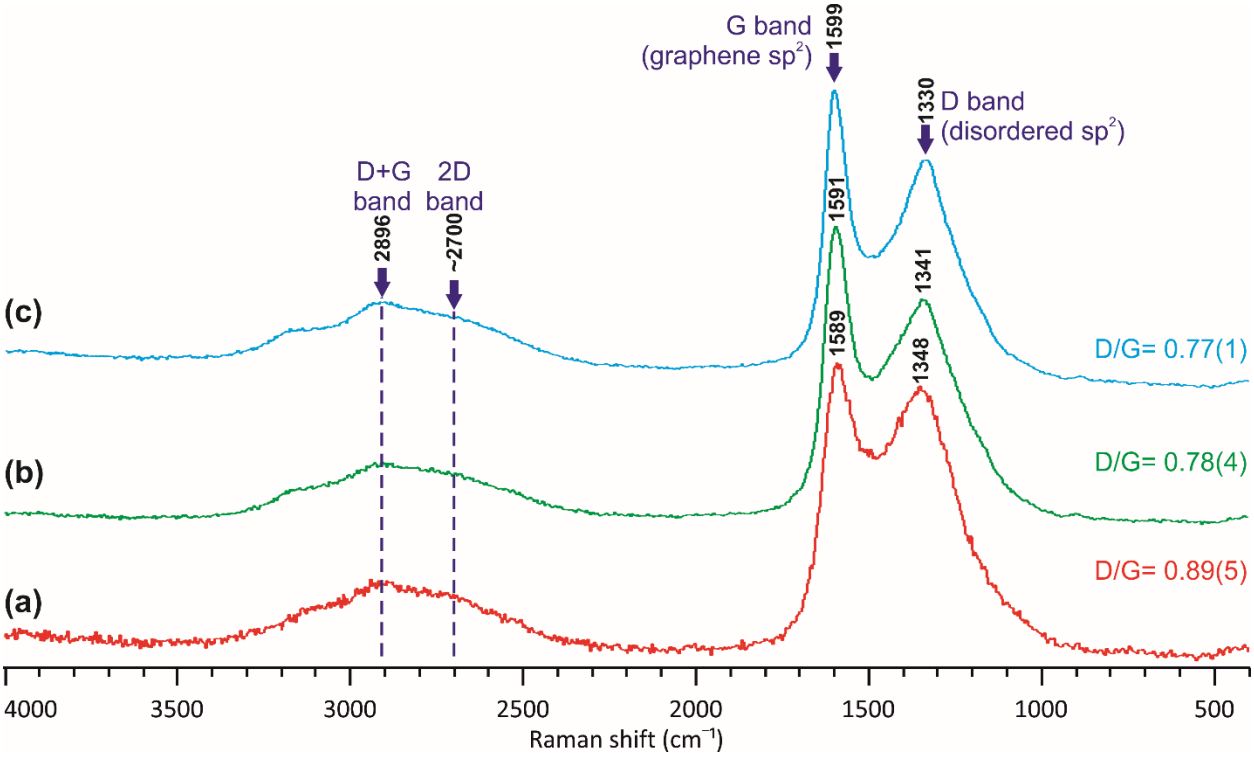

Figure S21. Raman spectra of the solid residues obtained in the course of thermal degradation (6 h in argon at 600 °C) of compound: (a) **1**, (b) **2**, and (c) **3**. D/G denotes a ratio of the D band intensity to the G band intensity (an error of estimation is given in parenthesis).

corresponding authors: maciej.debowski@pw.edu.pl; piogun@ch.pw.edu.pl

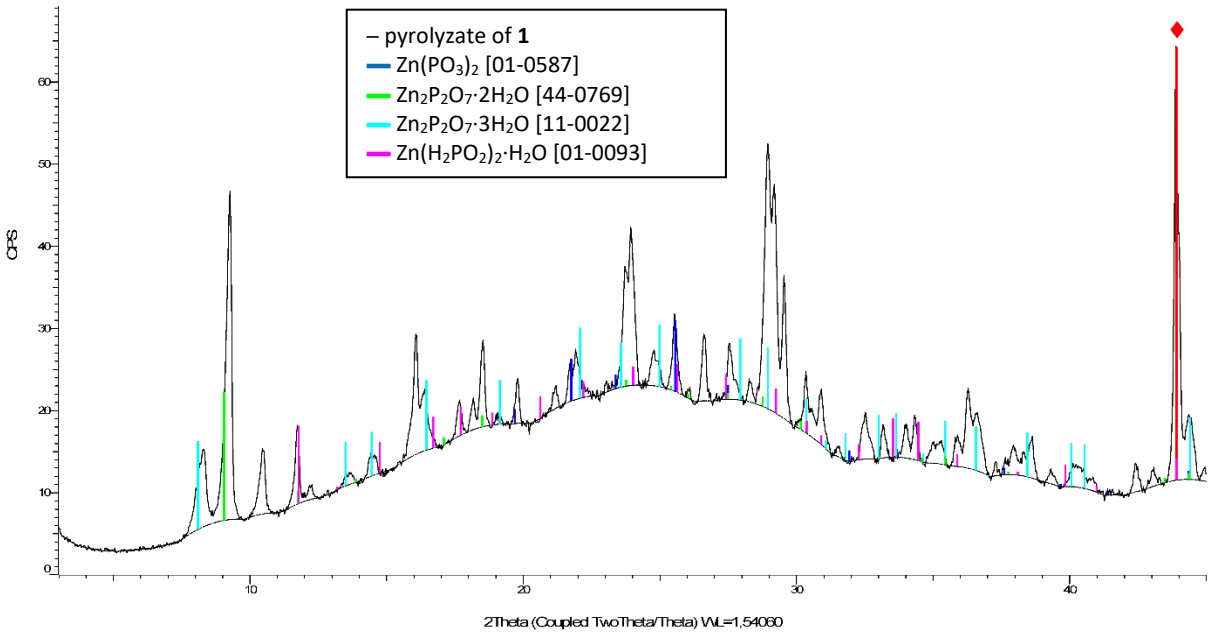

Figure S22. PXRD pattern of the solid residue obtained from thermal decomposition of compound **1** carried out for 6 h in argon at 600 °C (black line): the reflection around 44° (denoted with ♦) results from diamond powder used as an internal standard. Reflections characteristic of crystal phases of some selected condensed zinc phosphates or their hydrates are indicated with the coloured bars, together with their respective Powder Diffraction File numbers (in square brackets).

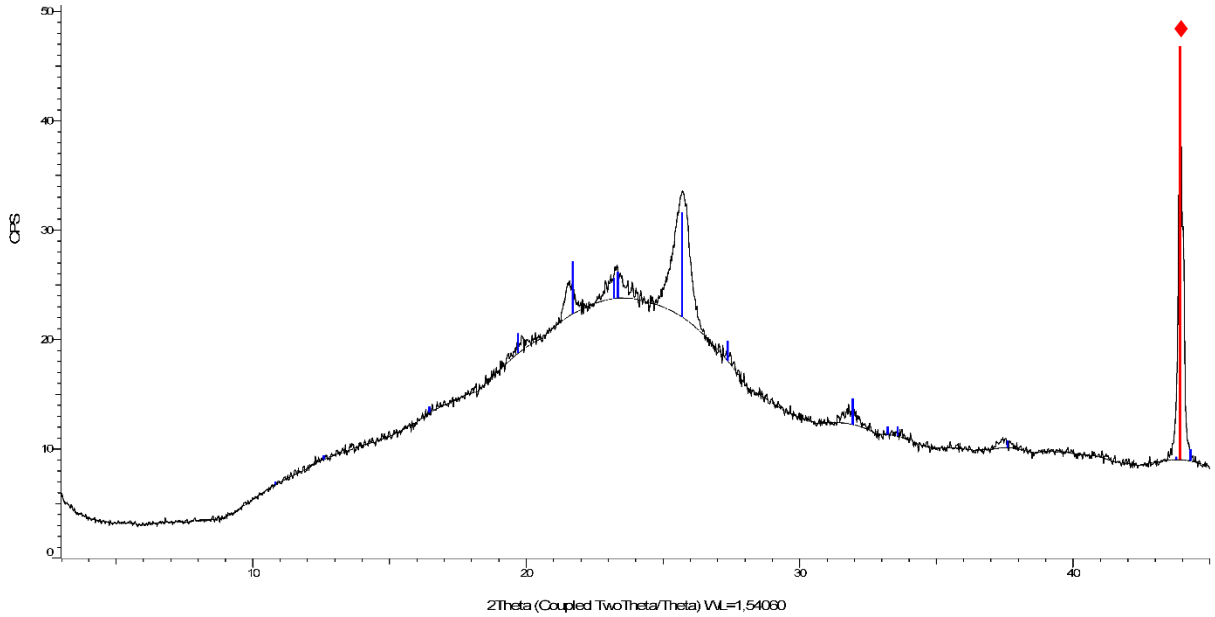

Figure S23. PXRD pattern of the solid residue obtained from thermal decomposition of compound **2** carried out for 6 h in argon at 600 °C (black line): the reflection around 44° (denoted with ♦) results from diamond powder used as an internal standard. Reflections characteristic of $Zn(PO_3)_2$ crystal phase [Powder Diffraction File No 30-1488] are indicated with dark blue bars.

corresponding authors: maciej.debowski@pw.edu.pl; piogun@ch.pw.edu.pl

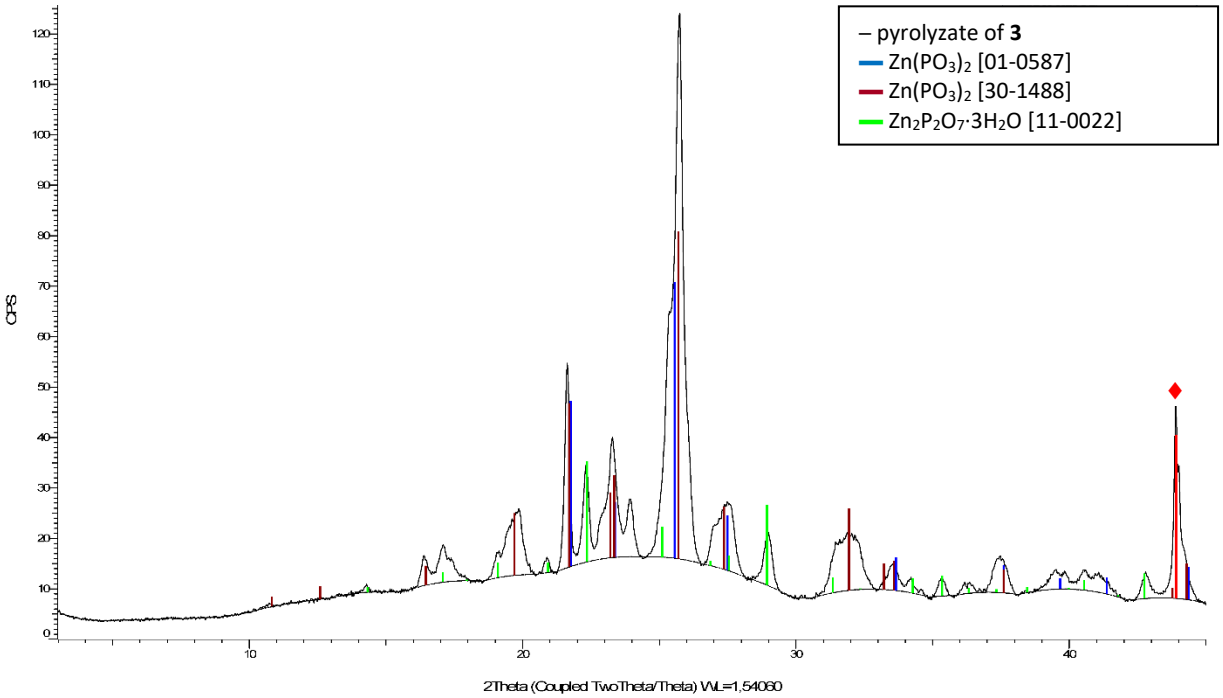

Figure S24. PXRD pattern of the solid residue obtained from thermal decomposition of compound **3** carried out for 6 h in argon at 600 °C (black line): the reflection around 44° (denoted with ♦) results from diamond powder used as an internal standard. Reflections characteristic of crystal phases of some selected condensed zinc phosphates are indicated with the coloured bars, together with their respective Powder Diffraction File numbers (in square brackets).

corresponding authors: maciej.debowski@pw.edu.pl; piogun@ch.pw.edu.pl

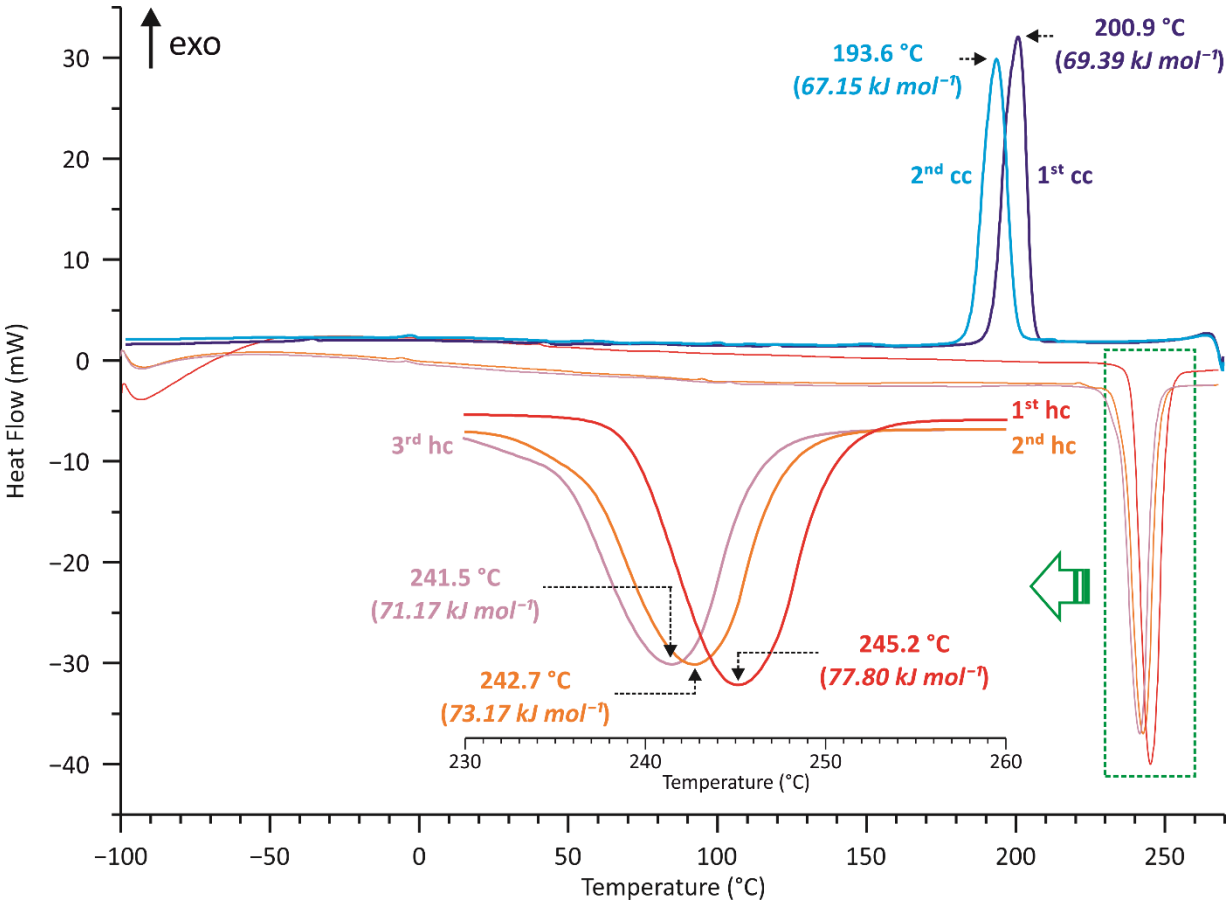

Figure S25. DSC traces of compound **1**. Enthalpies of the first–order transitions are given in parentheses. Heating (—, — or —) and cooling (— and —) runs are depicted. Heating/cooling rates of 10 °C min^{-1}. Abbreviations: **1st hc**, **2nd hc** and **3rd hc** – first, second and third heating curve, respectively; **1st cc** and **2nd cc** – first and second cooling run curve.

corresponding authors: maciej.debowski@pw.edu.pl; piogun@ch.pw.edu.pl

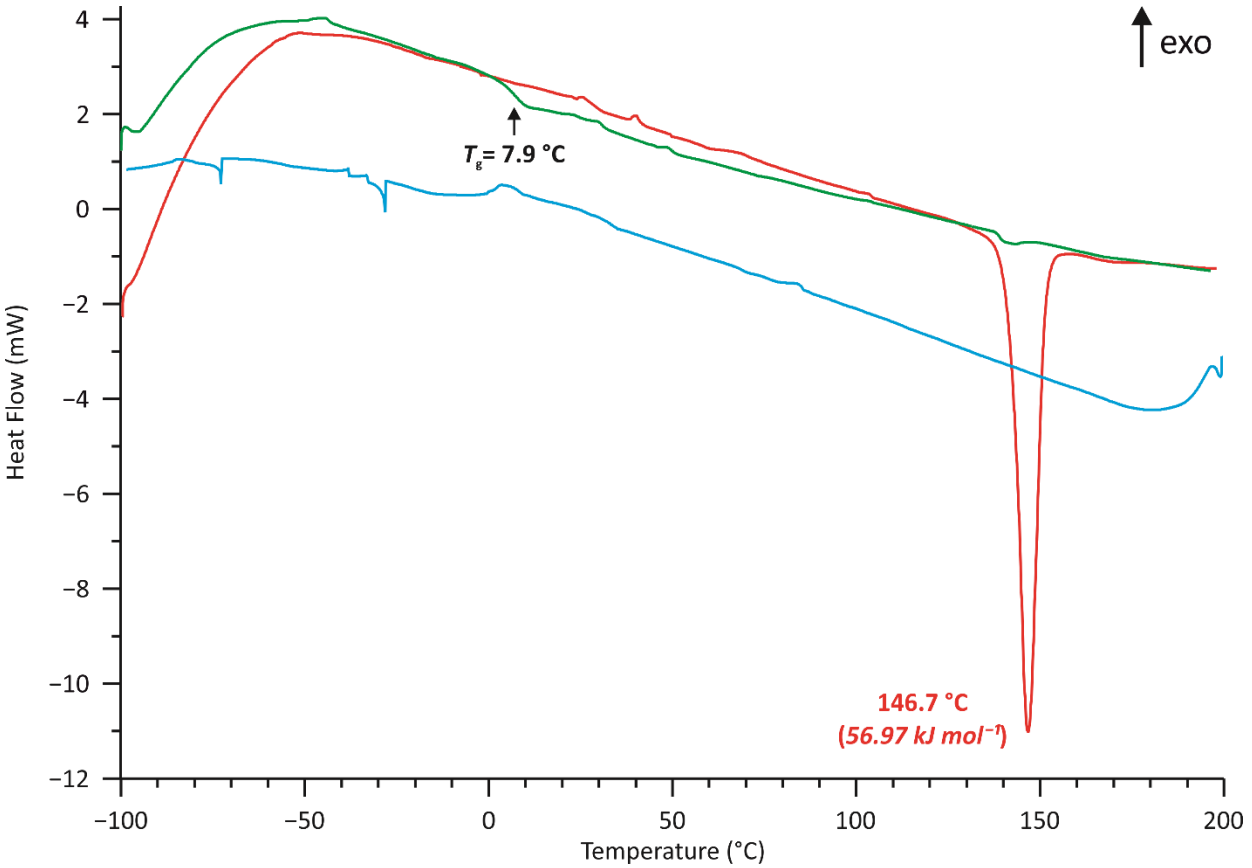

Figure **S26**. DSC traces of compound **3**: 1st heating (—), cooling (—) and 2nd heating (—) runs are depicted. Heating/cooling rates of 10 °C min^{-1}. Enthalpy of the first–order transition is given in parentheses. Abbreviation: T_g – glass transition temperature.

corresponding authors: maciej.debowski@pw.edu.pl; piogun@ch.pw.edu.pl

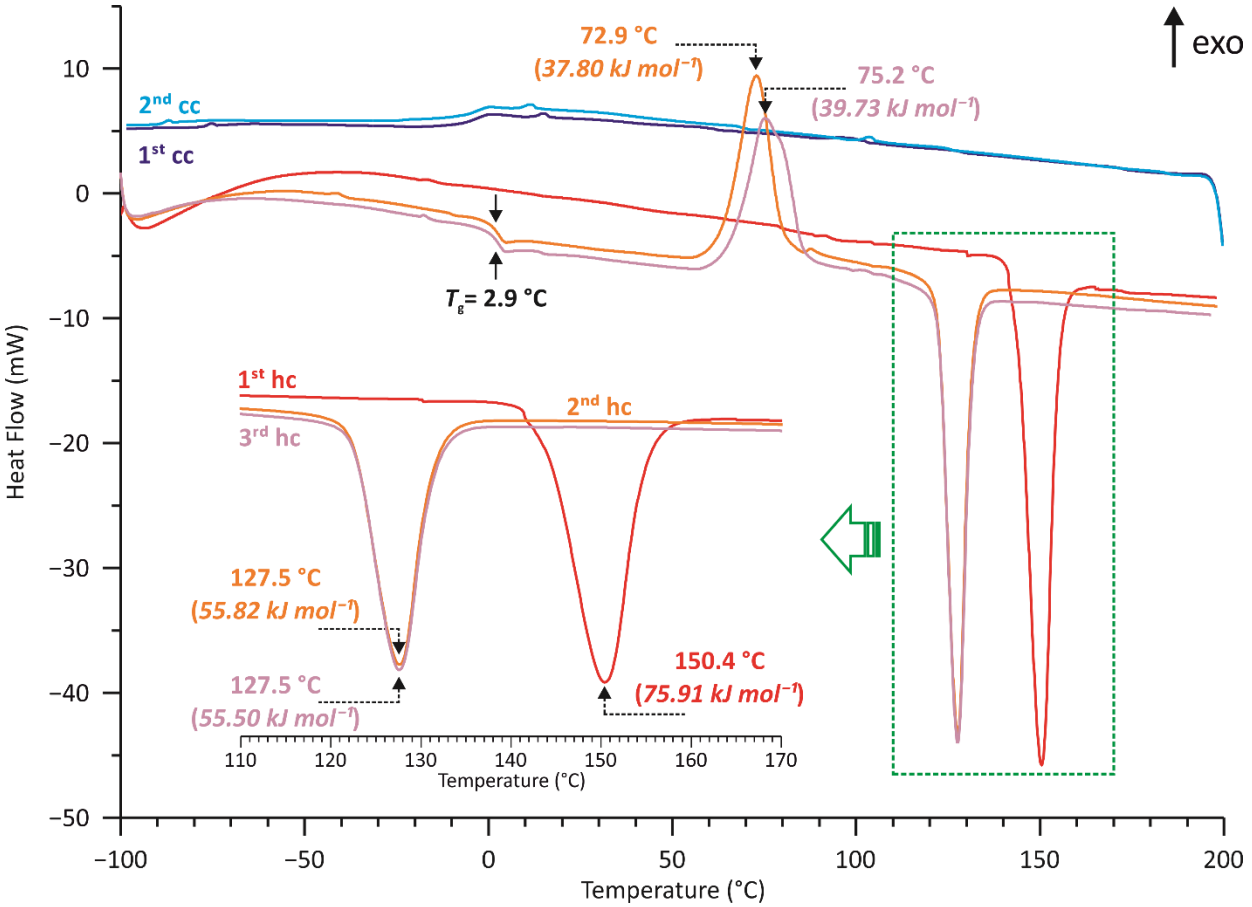

Figure **S27.** DSC traces of compound **2**. Enthalpies of the first–order transitions are given in parentheses. Heating (—, — or —) and cooling (— and —) runs are depicted. Heating/cooling rates of 10 °C min^{-1}. Abbreviations: **1st hc**, **2nd hc** and **3rd hc** – first, second and third heating curve, respectively; **1st cc** and **2nd cc** – first and second cooling run curve; T_g – glass transition temperature.

corresponding authors: maciej.debowski@pw.edu.pl; piogun@ch.pw.edu.pl

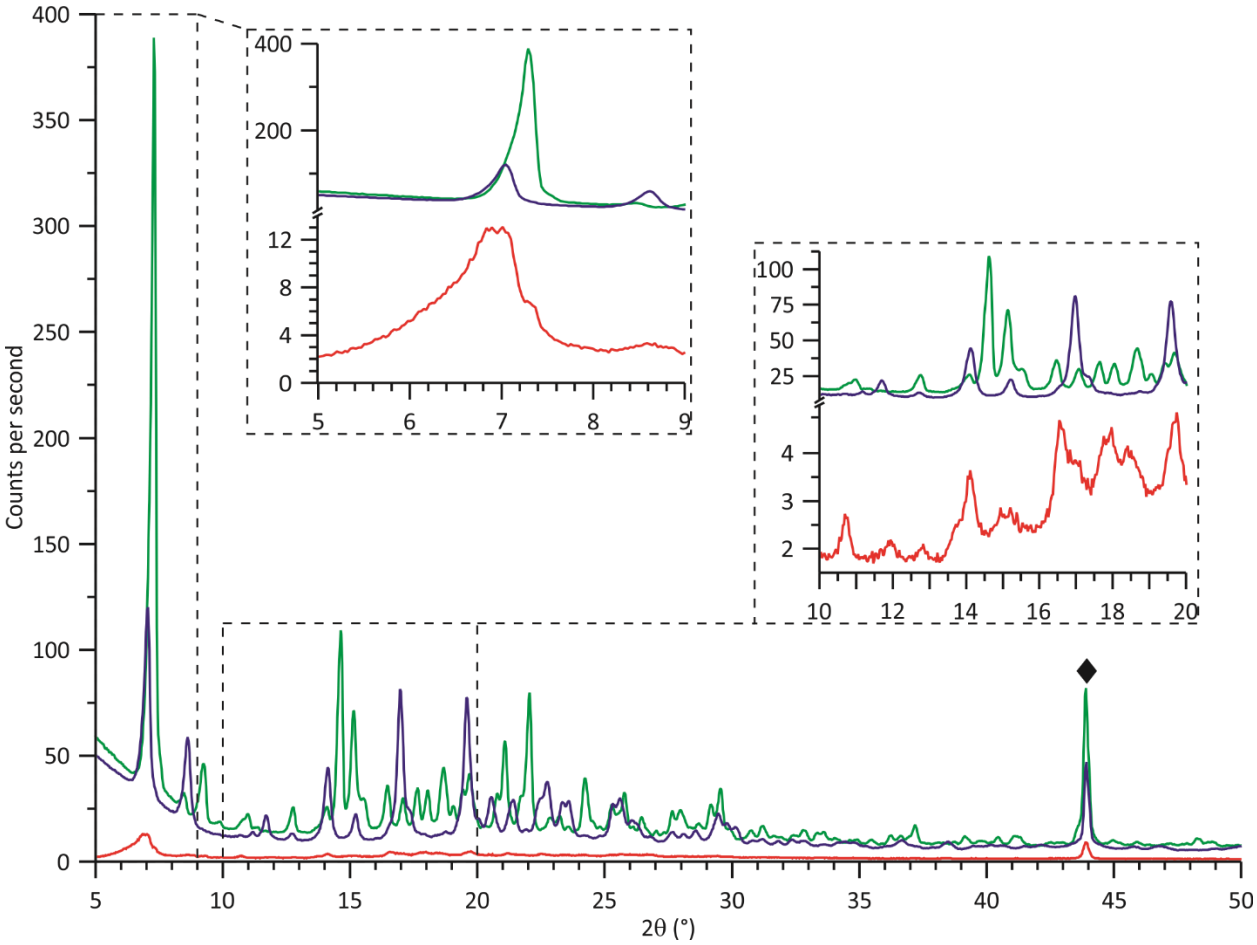

Figure **S28.** The experimental PXRD patterns of compound **2** recorded at room temperature: before thermal treatment (—), after conditioning at 160 °C for 3 h (—), and with additional conditioning at 90 °C (—). The reflection around 44° (denoted with ♦) results from diamond powder used as an internal standard

corresponding authors: maciej.debowski@pw.edu.pl; piogun@ch.pw.edu.pl

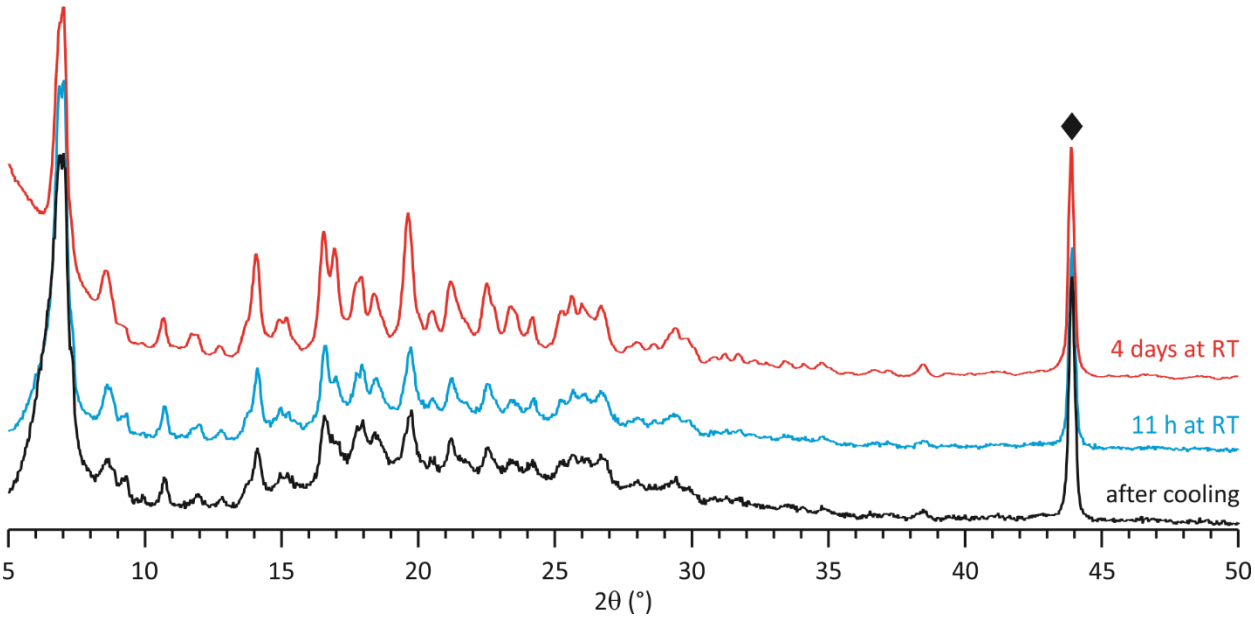

Figure **S29.** The experimental PXRD patterns recorded at room temperature after conditioning compound **2** at 160 °C for 3 h – sample measured: immediately after cooling to room temperature (—) and after 11 h (—) or 4 days (—) at room temperature. The diffractograms were normalized between 0 and 1. The reflection around 44° (denoted with ♦) results from diamond powder used as an internal standard.

corresponding authors: maciej.debowski@pw.edu.pl; piogun@ch.pw.edu.pl